Deep-Sea Research II 58 (2011) 1798–1818

Contents lists available at ScienceDirect

Deep-Sea Research II

journal homepage: www.elsevier.com/locate/dsr2

Export of Labrador Sea Water from the subpolar North Atlantic: A Lagrangian perspective

Amy Bower[a,*], Susan Lozier[b], Stefan Gary[b]

[a] Department of Physical Oceanography, Woods Hole Oceanographic Institution, Woods Hole, MA 02543, USA
[b] Earth and Ocean Sciences, Nicholas School of the Environment, Duke University, Durham, NC 27709, USA

ARTICLE INFO

Article history:
Received 12 October 2010
Accepted 12 October 2010
Available online 27 January 2011

Keywords:
Deep Western Boundary Current
Floats
Labrador Sea Water
Boundary currents
North Atlantic Current

ABSTRACT

Results from 59 acoustically tracked RAFOS floats obtained during 2003–2008 are analyzed here to study the spreading pathways of Labrador Sea Water (LSW) from the subpolar to subtropical North Atlantic. An earlier paper based on a subset of these float data presented evidence of a potentially important interior pathway for the southward spreading of LSW. Here those results are reinforced with the full data set and new information on LSW pathways around the Grand Banks is presented. About 70% of the RAFOS floats were expelled into the ocean interior east of the Grand Banks and meandered slowly eastward toward the mid-Atlantic ridge, a pathway observed previously with profiling floats. Less than 10% was advected continuously around the Grand Banks by the Deep Western Boundary Current (DWBC). A larger fraction (~17%) drifted into the subtropical interior from the Tail of the Grand Banks, suggesting that this pathway is at least if not more important than the DWBC pathway for the export of LSW to the subtropics. RAFOS floats released closest to the continental slope at 700 m depth were more likely to rapidly reach subtropical latitudes, mainly because they drifted through Flemish Pass, a 1100 m deep channel between the Grand Banks and the Flemish Cap, which protects fluid parcels from being swept off the continental slope by meanders of the North Atlantic Current. A statistical comparison of the RAFOS trajectories with more than 5000 simulated floats obtained from the Family of Linked Atlantic Models Experiment (FLAME) high-resolution ocean general circulation model reveals a similar pattern of LSW spreading. The RAFOS and simulated floats are also used to show that contrary to a previous modeling study, the isobaric RAFOS floats do not underestimate the amount of LSW that continuously follows the DWBC around the Grand Banks compared to isopycnal floats. These results have implications for the connectivity of the deep limb of the Atlantic Meridional Overturning Circulation between the subpolar and the subtropical North Atlantic.

1. Introduction

Since Henry Stommel and colleagues predicted on theoretical grounds the existence of a deep, western-intensified boundary current transporting cold dense water from the northern North Atlantic and the Antarctic (Stommel and Arons, 1960a, 1960b), observational evidence for such a current has steadily increased, especially in the North Atlantic. Measurements of potential vorticity, temperature and salinity anomalies, chlorofluorocarbons and other tracers have consistently shown a narrow vein of North Atlantic Deep Water ((NADW), including overflow waters from the Nordic Seas and convectively formed Labrador Sea Water (LSW)) hugging the continental slope of the western North Atlantic from the subpolar region to the equator (e.g., Talley and McCartney, 1982; McCartney, 1992; Doney and Jenkins, 1994; Smethie et al., 2000; Rhein et al., 2002; Stramma et al., 2004; Kieke et al., 2009, 2006; Dengler et al., 2006). Also, direct current measurements made at numerous locations along the western boundary of the North Atlantic always show a mean equatorward flow over the slope, coincident with the NADW tracer signature (e.g., Dengler et al., 2006; Pickart and Watts, 1990; Bryden et al., 2005; Fischer et al., 2004; Schott et al., 2004; 2006; Cunningham et al., 2007). From these and other observations an understanding developed of the North Atlantic Deep Western Boundary Current (DWBC) as the primary conduit for the southward transport of NADW, sometimes referred to as the deep limb of the "great ocean conveyor" (Broecker, 1991), an integral component of Earth's climate system.

It was therefore somewhat surprising when, in the 1990s, two float studies in the western subpolar North Atlantic showed no evidence of a continuous DWBC[1] connecting the subpolar to the

* Corresponding author.
E-mail address: abower@whoi.edu (A. Bower).

[1] In this paper, we use DWBC to refer to all the equatorward flow over the continental slope, not just the bottom-intensified flow transporting overflow waters.

0967-0645/$ - see front matter © 2011 Elsevier Ltd. All rights reserved.
doi:10.1016/j.dsr2.2010.10.060

subtropical regions of the North Atlantic. Profiling floats, which surface periodically to fix their position (Davis et al., 1992), exiting the Labrador Sea in the DWBC in the depth range of Labrador Sea Water (400–1500 m) were all quickly expelled from the DWBC east of the Grand Banks and the Flemish Cap and drifted mainly eastward along the subpolar–subtropical gyre boundary, defined by the eastward-flowing branches of the North Atlantic Current ((NAC); see Fig. 1A for circulation features and geographic locations) (Lavender et al., 2000, 2005; Fischer and Schott, 2002). Hydrographic and tracer studies have shown that this eastward pathway is another of several spreading axes of LSW (Talley and McCartney, 1982; Rhein et al., 2002), but the complete lack of evidence of a continuous pathway southward along the western boundary in the float trajectories ran counter to our understanding of the DWBC as the dominant export pathway for recently ventilated water from the subpolar North Atlantic.

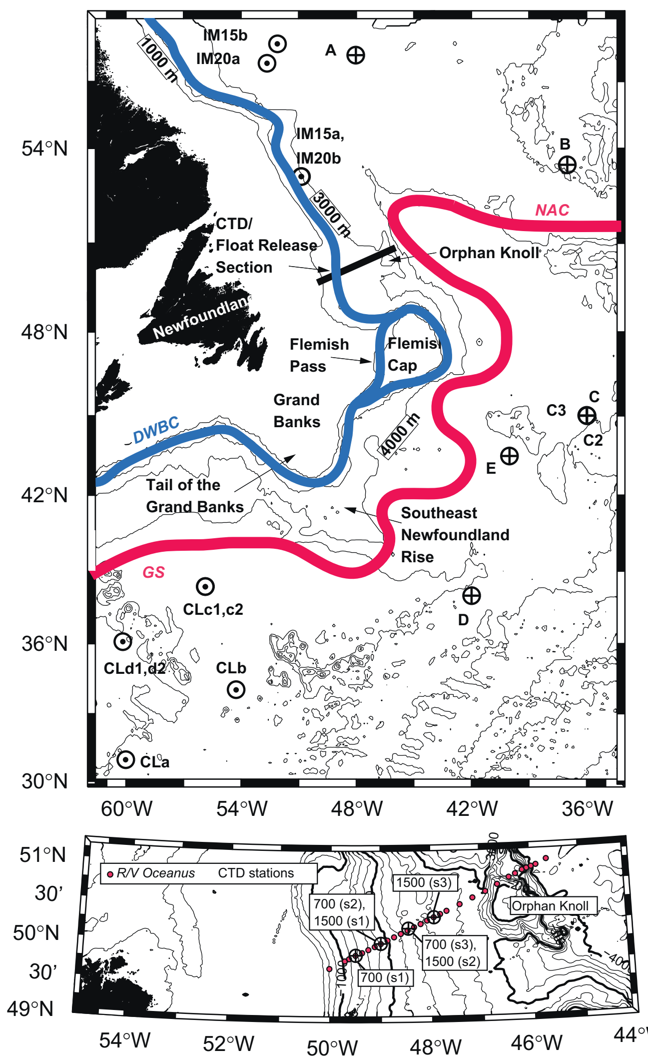

Fig. 1. (A) Schematic diagram of the major currents in the western North Atlantic in the vicinity of the Grand Banks of Newfoundland, including geographical locations referred to in the text. Open circles with central dot indicate the locations of the principle sound sources used for tracking the RAFOS floats, A-E maintained by the Woods Hole Oceanographic Institution and IfM by the Institut fur Meereskunde in Kiel, Germany. Isobaths are drawn at 1000 m intervals. (B) Expanded view of the float release section. Small circles show the positions of CTD stations occupied during the first float deployment cruise in July 2003. Repeated float releases were made at the positions indicated by the four large symbols according to the information in the boxes. S1–S3 refer to the cross-slope release sites for the 700 and 1500 m floats. Isobaths are drawn every 250 m and highlighted every 1000 m.

To resolve this apparent contradiction in Eulerian and Lagrangian views of the importance of the DWBC in the southward spreading of LSW, several questions needed to be addressed. First, did the profiling floats accurately follow LSW in the Grand Banks region where the DWBC and NAC flow close together but in opposite directions (Fig. 1A)? Fischer and Schott (2002) showed that most of the profiling float displacements from the DWBC into the interior occurred at depth, not while the floats were at the surface, and argued that the profiling did not bias the floats toward being expelled from the DWBC. On the other hand, Getzlaff et al. (2006) (hereafter G06) simulated the behavior of various float types in this region in a high-resolution numerical model of the North Atlantic and found that profiling did impact the ability of floats to follow fluid parcels along the DWBC pathway. Second, were the profiling floats biased by their launch site to follow the eastward pathway? Most of the profiling floats that exited the Labrador Sea in the DWBC were either entrained into the DWBC from the Labrador Sea interior or released on the offshore half of the current (Lavender et al., 2000; Fischer and Schott, 2002), which could precondition them for rapid expulsion from the DWBC. Third, could there be low-frequency variability in the dominance of the various LSW spreading pathways, perhaps related to strength of deep convection in the Labrador Sea and/or variable wind forcing?

In 2003, a new float study, called Export Pathways from the subpolar North Atlantic (ExPath), was undertaken to address these questions and further investigate the spreading pathways of LSW from the subpolar to subtropical North Atlantic. Subsurface floats were sequentially released in the DWBC at 50°N at two depths within LSW during 2003–2006 (see Fig. 1A and B for float release sites). To avoid a possible bias in trajectories related to profiling, acoustically tracked RAFOS floats (Rossby et al., 1986), which surfaced only once at the end of their two-year mission to transmit data, were used in the current study. To avoid a possible bias related to float launch position, the floats were released as close to the continental slope as possible without the risk of grounding. A total of 55 two-year RAFOS float trajectories and accompanying temperature and pressure records, about half at 700 m and half at 1500 m, were obtained.

Based on the first 40 RAFOS floats from this program, Bower et al. (2009) (hereafter B09) showed that most of the floats followed a path similar to that of the profiling floats, namely from the DWBC east of the Grand Banks eastward along the subpolar–subtropical gyre boundary. A small fraction of the floats ($<10\%$) followed the DWBC continuously around the Grand Banks, which none of the profiling floats had done. The most surprising result however was that a larger fraction was expelled from the DWBC at the southern tip of the Grand Banks and drifted southward into the subtropical region, suggesting that there is an interior pathway for LSW to spread rapidly southward through the subtropics that is as or more important than the DWBC pathway. Analysis of more than 7000 simulated trajectories (hereafter called "e-floats") from a high-resolution North Atlantic general circulation model also revealed this interior pathway, and the longer simulated trajectories (up to fifteen years) suggested that the interior pathway rejoins the DWBC south of Cape Hatteras.

Here we reinforce the results of B09 using the full RAFOS float data set and address new questions not dealt with in the previous study. First, how well, statistically speaking, do the simulated trajectories reproduce the LSW spreading pathways observed with the RAFOS floats? Second, how does the chance that a float (or fluid parcel) will be exported rapidly to the subtropics depend on depth and cross-slope position? Third, did the isobaric (constant pressure) property of the RAFOS floats used in this study bias them toward being expelled from the DWBC and entrained by the Gulf Stream and North Atlantic Current? Addressing these questions, we strengthen the argument for an important interior pathway for the southward spreading of LSW that has implications for how the ocean interior is ventilated and the ultimate impact of oceanic climate change signals on the circulation.

The structure of this paper is as follows. In Section 2, we review the RAFOS float data set and construction of the simulated trajectories. Section 3.1 describes the release of RAFOS floats within the cross-stream structure of the DWBC at 50°N, Section 3.2 shows large-scale spreading pathways of the full RAFOS float data set, Section 3.3 provides a statistical comparison with the simulated trajectories, Section 3.4 examines the effect of float depth and cross-slope location on spreading pathway and Section 3.5 addresses the issue of isopycnal versus isobaric floats drifting around the Grand Banks. The results are discussed and summarized in Section 4.

2. Data and methods

2.1. RAFOS floats

The RAFOS floats used in this study were released in the DWBC near 50°N (see Fig. 1A for float release site) in subsets of nominally 6 floats every three months between July 2003 and November 2006 for a total of 13 separate releases. All but the first release were made during occupation of the "Bonavista" repeat hydrographic section by the Northwest Atlantic Fisheries Centre in St. John's, Newfoundland. This Canadian repeat hydrographic section runs from Cape Bonavista on the Newfoundland coast, across the shelf and slope to Orphan Knoll, a seamount located northwest of Flemish Cap. Compared to other nearby locations, the continental slope is relatively gentle along this section. The sill depth between the shelf and the Orphan Knoll is about 2800 m deep (Fig. 1B).

Each float was tracked acoustically using moored sound sources (see Fig. 1A for positions of primary sources used) for two years and collected temperature, pressure and acoustic travel time information once daily (see Rossby et al., 1986 for technical details). The floats were "isobaric" (Swift and Riser, 1994) and half were ballasted for 700 m and the other half for 1500 m. The floats were released at four positions across the continental slope between the 1400 and 2600 m isobaths (Fig. 1B). Of the 76 floats released, 59 returned data (32 from 700 m and 27 from 1500 m), yielding 59 two-year displacement vectors and 55 trajectories. More details regarding the RAFOS floats and data processing can be found in Furey and Bower (2009).

Fig. 2 shows the data return for the 700 (red) and 1500 (blue) floats as functions of release group, season, year and release site. Data return was variable through the program, with a minimum of 1/6 from group 3 (February 2004) and a maximum of 8/8 from group 12 (April 2006). Data return from spring, summer and fall releases was relatively uniform, but there were fewer successful winter releases. The winter releases were accomplished using a "float park", where floats are temporarily anchored to the sea floor during the fall deployment and programmed to release their anchors and begin their drifting missions the following February (Zenk et al., 2000). The low winter return reflects the overall riskier nature of this release method (Furey and Bower, 2009).

The first year saw the lowest number of returns (16) and the third year the most (23). The data return was the highest for the inshore release sites and decreased offshore because we favored the inshore sites whenever there were not enough floats to populate all the sites or if there were extra floats on a given deployment.

2.2. Simulated floats

The numerical trajectories used in this study were generated using the high-resolution (1/12°) general circulation model FLAME (Family of Linked Atlantic Models Experiment), which was based on the Geophysical Fluid Dynamics Laboratory MOM2.1 code and modified as part of the FLAME project (Dengg et al., 1999).

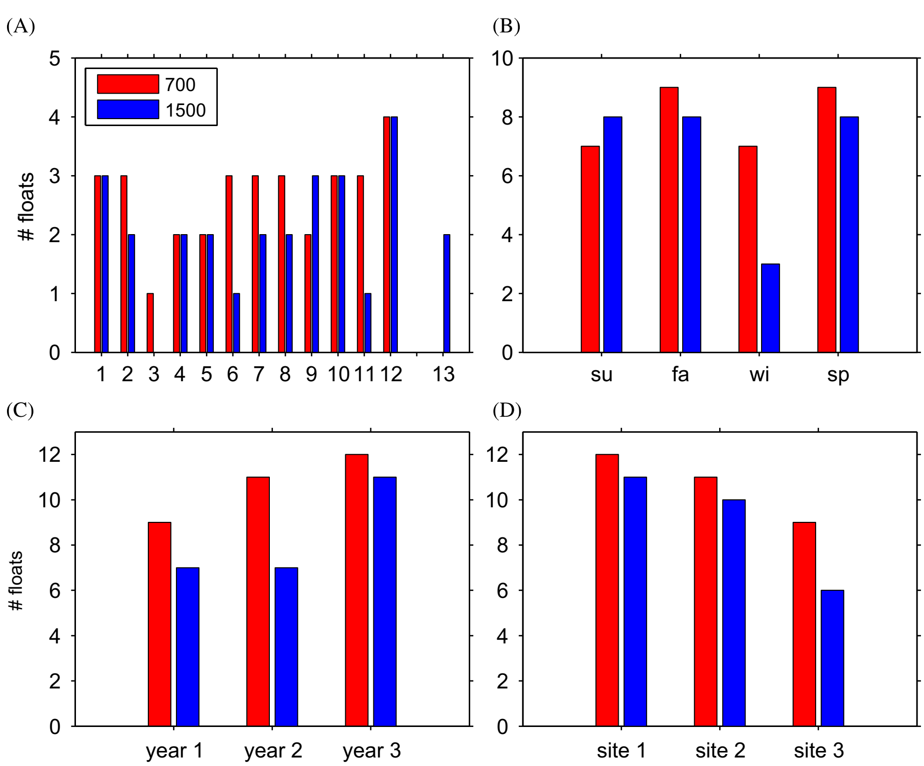

Fig. 2. Number of RAFOS float trajectories obtained during the ExPath program by (A) setting, (B) season, (C) year and (D) release site for 700 m (red) and 1500 m (blue) floats.

Following a ten-year spin-up from rest with climatological forcing based on the climatology of the European Center for Medium-Range Weather Forecasting (ECMWF), this model was run with interannually varying wind and thermohaline forcing consisting of monthly anomalies computed from the NCEP/NCAR reanalysis data (Kalnay et al., 1996) for the period 1987–2004 (see Willebrand et al., 2001; Eden and Boening, 2002; Boening et al., 2006 for details of forcing, boundary conditions and mixing parameterizations). Model output consists of three-dimensional snapshots of horizontal velocity, temperature and salinity fields over the domain on a 1/12° Mercator grid. In the vertical, the domain was split into 45 z-coordinate levels. The vertical velocity was computed from the horizontal velocity by requiring that the local divergence of the three-dimensional velocity field be zero throughout the model domain.

Output from FLAME has been compared to observations in several studies focused mainly on the subpolar and tropical Atlantic. Eden and Boening (2002) assessed the performance of FLAME in reproducing the mean circulation and eddy kinetic energy in the Labrador Sea (north of 48°N). They found good agreement in the width, maximum velocity and transport of the mean boundary currents (West Greenland and Labrador Currents) and with the spatial distribution, magnitude and seasonality of surface eddy kinetic energy (EKE). Boening et al. (2006) showed that FLAME reproduced the gradual increase in sea surface height following the switch in the sign of the North Atlantic Oscillation (NAO) index after 1994 (Hakkinen and Rhines, 2004) based on altimetric observations, as well as the decadal trends in the transport of the DWBC observed with current meters at 53°N (Dengler et al., 2006). G06 found good agreement between FLAME and direct observations of the mean western boundary current transport at 53 and 43°N, as well as with subsurface EKE levels at 43°N, where the model captured about 90% of the observed variability at 1500 m depth at the DWBC–NAC transition.

There has been no systematic assessment to date of the model's performance in the region of the RAFOS float observations. In the Appendix, we provide a basic comparison between mean surface currents and EKE in FLAME and in observations for the region 35–54°N, 60–35°W, that is, the region around the Grand Banks. This is not an exhaustive assessment of FLAME in this region, but provides important background information on the model's ability to reproduce the location of the major currents and the strength of the time-dependent circulation, both of which will impact the spreading pathways of the numerical trajectories.

The numerical trajectories (hereafter referred to as e-floats) were computed by integrating for 15 years the three-day velocity snapshots using a method described by Kröger (2001). Two e-float "experiments" were conducted. The first was set up to simulate the release of RAFOS floats at 50°N and was first described by B09. In this case, the velocity fields from FLAME model years 1994, 1996 and 1998, repeated sequentially, were used to compute the numerical trajectories. These years represent a variety of forcing states as indicated by the NAO index. Twenty e-floats were "released" every three days over the course of the first three years at sites bracketed by the most inshore and offshore RAFOS float release sites (see Section 3.1 below for model release sites). This generated a total of 364 e-float settings and 7280 trajectories. The primary e-float data set analyzed here was constructed using the full three-dimensional velocity fields to simulate as closely as possible the three-dimensional (3D) motion of fluid parcels along isopycnals. A second e-float data set was produced with the identical initialization distributions as for the 3D case but using only the model's horizontal velocity components (2D) in order to simulate movement of isobaric floats. Note that throughout the study, "700 m" and "1500 m" e-floats refer to the depth of the e-floats at release—the 3D e-floats change depth along their trajectories, reflecting the three-dimensional velocity field.

It will be shown below that the float trajectories are sensitive to launch site and depth, so the 3D and 2D e-float trajectories were subsampled to mimic the release distribution and depth distribution of the RAFOS floats (Fig. 2). The total number of e-float trajectories in Experiment 1 was reduced from 7280 to 5360 as a result of this conditional sampling.

Experiment 2 was performed using an e-float release site closer to the Tail of the Grand Banks, specifically at 43°N, to focus on the physical processes there and to make a comparison with a similar experiment reported by G06. In one case, the mean velocity field from the years 1994–1998 was used to calculate fifteen-year trajectories of 8317 e-floats released in the depth range 700–2000 m along 43°N between 50 and 46°W. Only those e-floats that were released in the DWBC, identified by a southward drift over the first three days after release, were retained. In the second case, the time-dependent velocity fields for the years 1994–1998, repeated sequentially as in the first experiment, were used to calculate the fifteen-year trajectories of sets of 88 e-floats released every 15 days, generating a total of 8360 simulated trajectories. Again, the total set was subsampled to include only those floats that drifted initially southward in the DWBC. The two experiments are summarized in Table 1.

3. Results

3.1. Release sites of RAFOS floats relative to DWBC structure

Before describing the large-scale LSW spreading pathways based on the RAFOS floats, it is important to have a thorough understanding of where they were released relative to the hydrographic and current structure of the DWBC at 50°N. Fig. 3 shows cross-sections of potential temperature, salinity, sigma-0 and the along-isobath component of absolute geostrophic velocity from the CTD and hull-mounted ADCP measurements collected during the first RAFOS float deployment cruise in July 2003 (see Fig. 1B for station positions). The absolute geostrophic velocity was determined by matching the depth-averaged relative geostrophic velocity over the upper 300 m to the depth-averaged

Table 1
Summary of two numerical float experiments conducted to study the Lagrangian spreading pathways of LSW within FLAME.

	Release latitude	Model velocity years used	Release interval (days)	Total number of trajectories	Total number analyzed
Experiment 1					
Time-dependent	50°N	1994, 1996, 1998	3	7280	5360
Experiment 2					
Mean	43°N	1994–1998 mean	N/A	8317	3004 (3D) 3001 (2D)
Time-dependent	43°N	1994–1998	15	8360	3646 (3D) 3630 (2D)

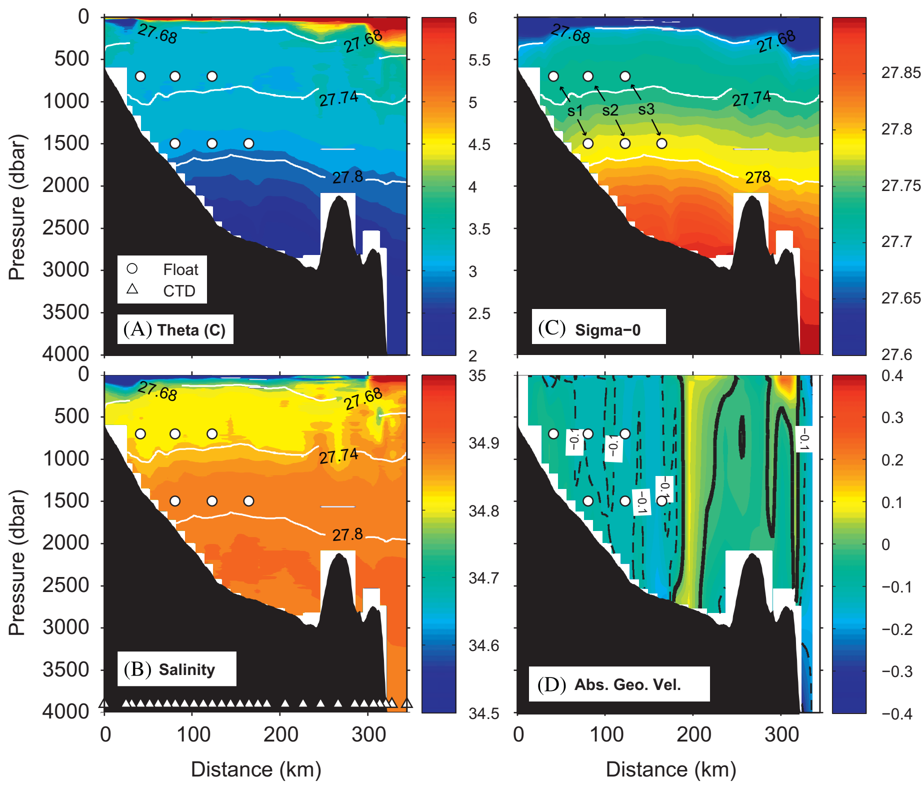

Fig. 3. Vertical sections of (A) potential temperature, (B) salinity, (C) potential density referenced to the surface and (D) along-isobath absolute geostrophic velocity from the CTD/ADCP section occupied during the first RAFOS float deployment cruise in July 2003. The observer is looking northward, with the continental shelf to the left and Orphan Knoll to the right. See Fig. 1B for station positions. The open circles indicate the positions of the RAFOS float deployments at 700 and 1500 m. S1–S3 mark the inshore, middle and offshore release sites at each depth. Upward triangles show CTD station positions, and white contours denote layer boundaries for Upper and Classical LSW.

absolute velocity obtained from the hull-mounted ADCP. Selected isopycnals recently used to define the boundaries of Upper LSW (27.68–27.74 kg m^{-3}) and Classical LSW (27.74-27.80 kg m^{-3}) are shown for reference (Kieke et al., 2006).

Potential temperature and salinity were essentially homogeneous across the portion of the continental slope where the RAFOS floats were deployed (open circles), Fig. 3A and B. Potential temperature varied by only 0.04 °C at 700 and 1500 m (3.20–3.24 °C at 700 m, 3.04–3.08 °C at 1500 m), and there was no obvious trend at either depth. Salinity was similarly uniform. The lack of significant horizontal density gradients (Fig. 3C) is reflected in the velocity structure (Fig. 3D), which is relatively barotropic between the upper slope and the Orphan Knoll. Maximum southward speeds were 10–20 cm/s and were the strongest between the 1500 and 3000 m isobaths. This is the water depth range often reported for the core of the Deep Labrador Current (Dengler et al., 2006; Fischer and Schott, 2002; Lazier and Wright, 1993). This section did not cross the baroclinic Labrador Current, which is found inshore of the 1000 m isobath (Lazier and Wright, 1993). There was no apparent bottom-intensified velocity or tracer core at the LSW levels where the RAFOS floats were released. Near Orphan Knoll, more baroclinic structures associated with eddies of the NAC were present. Assuming that the hydrographic and velocity structure observed during July 2003 was representative of the conditions during other RAFOS float deployments, we conclude that the floats were released well within and span the tracer- and velocity-based definitions of the DWBC at the LSW level.

3.2. Large-scale LSW spreading pathways observed with RAFOS floats

Fig. 4A shows the trajectories of all 55 RAFOS floats (29 at 700 m, 26 at 1500 m), color-coded according to temperature observed along their path. In order to use the same color scale for the 700 and 1500 dbar floats, float temperature was converted to a normalized temperature anomaly, defined as $(T-T_i)/\delta T_{\max}$. T_i is each float's initial temperature, and $\delta T_{\max}$ is the maximum temperature range observed by the floats as a group, 6.4 °C at 700 dbar and 1.8 °C at 1500 dbar. Simply put, blue (red) indicates colder (warmer) float temperatures. Dashed lines indicate untrackable segments of the float trajectories, and upward triangles show surface position after two years.

Immediately after release, nearly all of the RAFOS floats drifted southward parallel to the isobaths over the continental slope, with a mean speed of 8 ± 4 cm s^{-1} and peak 48 h speeds of about 30 cm s^{-1}. About one-third of the 700 m floats (10/32) drifted through Flemish Pass, the 1100 m deep channel between the Grand Banks and the Flemish Cap (see Fig. 1A for location). Float tracking was not always possible within the Pass itself due to the blocking of sound signals by the Flemish Cap (which rises to within less than 200 m of the sea surface), but tracking resumed once the float emerged from the southern end of the pass. Almost all of the floats that did not go through Flemish Pass continued eastward along the northern flank of Flemish Cap, then turned southward along its steeper eastern flank, where the mean float speed increased to 16 ± 11 cm s^{-1}.

Most of the floats that did not go through Flemish Pass peeled away from the slope east of Flemish Cap and the Grand Banks and drifted into the interior, as nearly all of the profiling floats did in earlier studies (Fischer and Schott, 2002). As shown by Kearns and Rossby (1998), B09 and in Fig. A1, the NAC makes its closest approach to Flemish Cap at its southeast corner (about 47°N). B09 showed that this is where most of the RAFOS floats drifted away from the slope into the interior. The tangle of float trajectories east of the Grand Banks coincides with the local maximum in surface EKE associated with the eddies and meanders of the NAC

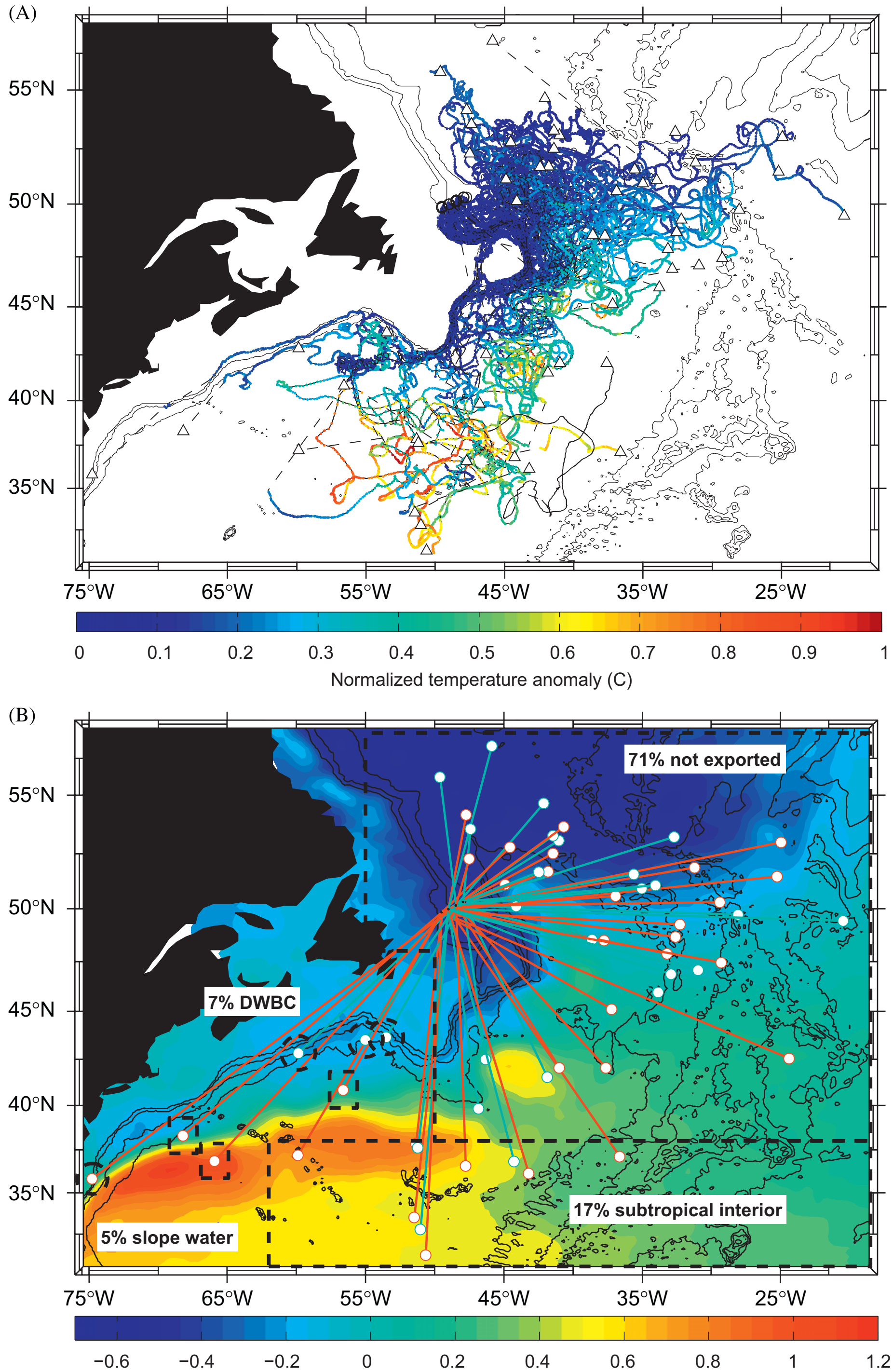

Fig. 4. (A) Trajectories of 55 RAFOS floats released at 50°N, 29 at 700 m depth and 26 at 1500 m. Daily positions are color-coded according to float temperature (see text). Triangles show surface positions two years after release. The 1000, 2000 and 3000 m isobaths are drawn. (B) Two-year displacement vectors for the trajectories in (A) plus four more for which acoustic tracking was not available. Colors indicate float depth, red for 700 m and cyan for 1500 m. Color shading indicates mean dynamic topography from AVISO (see the Appendix for details). Areas bounded by heavy dashed lines show four destinations for the floats two years after release, and the percentages of floats which ended up in each area: "not exported" (north of 38°N and east of 50°W); "subtropical interior" (south of 38°N and east of 62°W); "DWBC" (dashed circles); and "slope water" (dashed squares).

(Heywood et al., 1994; Rossby, 1996; Carr and Rossby, 2001; Fratantoni, 2001 and Figs. A3 and A4). The floats that remained east and north of Flemish Cap measured relatively cooler temperatures compared to those that drifted south of the Grand Banks (Fig. 4A), indicating that they had recirculated within the subpolar gyre. Some of the northern group crossed over the Mid-Atlantic Ridge into the eastern North Atlantic within two years after release, presumably along the path of the various eastward-flowing branches of the NAC (Fig. 1A).

A few RAFOS floats followed the DWBC pathway continuously around the Grand Banks and surfaced after two years over the continental slope west of the Grand Banks. The longest drift along this path took a 700 m float near to Cape Hatteras. Although more than what was observed with profiling floats (zero), the number still seems smaller than what we might have expected for the DWBC in light of the common understanding of the DWBC as the principal conduit for the southward spreading of recently ventilated water masses. These floats maintained relatively cool temperatures, indicating that they were being advected along the path of the DWBC.

As first reported by B09, a larger number of RAFOS floats followed an interior pathway into the subtropical region than followed the DWBC (Fig. 4A). The passage of these floats across the Gulf Stream and into the subtropical interior is confirmed by their warmer temperatures. The largest meridional displacements over two years (50–32°N) were observed in this group of floats, which B09 argued was an evidence of an important southward interior pathway for the spreading of LSW. This pathway was also evident in FLAME based on the trajectories of thousands of simulated e-floats (B09). More support for the interior pathway will be presented in the following sections.

Fig. 4B shows the two-year displacement vectors of the 55 floats in Fig. 4A plus four more for which only launch and surface positions were obtained, color-coded according to float depth. The vectors are superimposed on a map of mean absolute dynamic topography (MDT09; see the Appendix for details) from AVISO to illustrate the float spreading pattern relative to the large-scale surface circulation.

To quantify the importance of the various spreading pathways, the 59 RAFOS float displacement vectors have been grouped together according to their surface positions, which will be referred to as destination statistics. There are other methods to sort the float trajectories, but this one was simple and seemed to capture the major differences in the large-scale drift of the floats. All of the floats that surfaced north of 38°N and east of the Grand Banks and the Canadian Maritimes are categorized as "not exported", that is, they were not (yet) clearly exported from the subpolar region (Fig. 4A). This categorization is the least secure for the floats in the latitude range 38–50°N east of the Grand Banks, which surfaced among the various branches of the NAC, manifested as a broad eastward flow in the mean dynamic topography. For the purposes of this study however, only those floats that were clearly exported to the west or south of the Newfoundland Basin were categorized as "exported" in two years and the rest were considered to be "not exported". The exported group is divided into three subgroups: floats that surfaced over the continental slope west of the Grand Banks ("boundary current"), floats that surfaced south of 38°N and east of 62°W (subtropical interior) and those that surfaced in between the boundary current and the Gulf Stream ("slope water").

The destination statistics for the RAFOS floats are summarized in Fig. 5A. A large majority of the RAFOS floats (71%) were not exported within two years. This is an order of magnitude higher than the fraction of exported boundary current floats (7%). The subtropical interior pathway appears as the most important of the three export groups, making up 17% of all floats and 59% of the exported floats. These fractions are similar to those reported by B09 based on a subset of the full data set.

3.3. Statistical comparison between RAFOS and simulated trajectories

In B09, thousands of numerical float trajectories generated within FLAME also revealed an interior export pathway for LSW into the subtropical region. Here we attempt to quantify the similarity of the RAFOS and simulated trajectories. First, we consider the structure of the model DWBC at 50°N, where both the RAFOS and simulated floats were released, Fig. 6. The mean potential temperature, salinity, density and along-isobath velocity for the model years 1987–2004 are shown along with the release

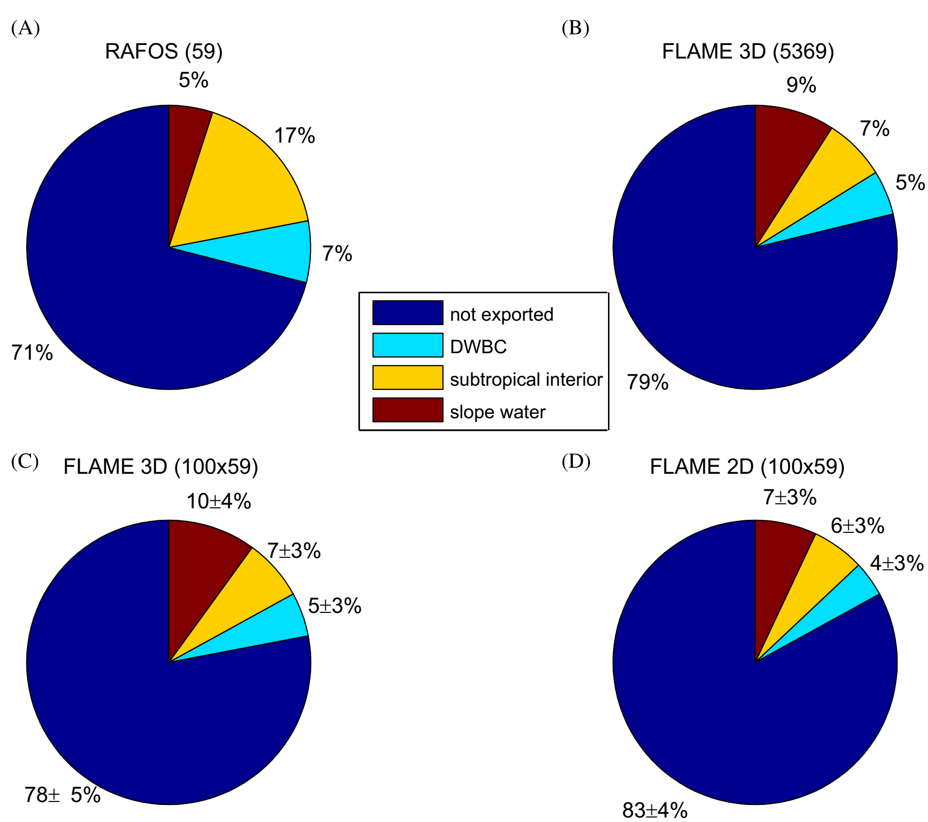

Fig. 5. Summary of destination statistics after two years for (A) 59 RAFOS floats, (B) 5360 3D e-floats, (C) 100 ensembles of 59 3D e-floats each, mean and standard deviation and (D) 100 ensembles of 59 2D e-floats each, mean and standard deviation.

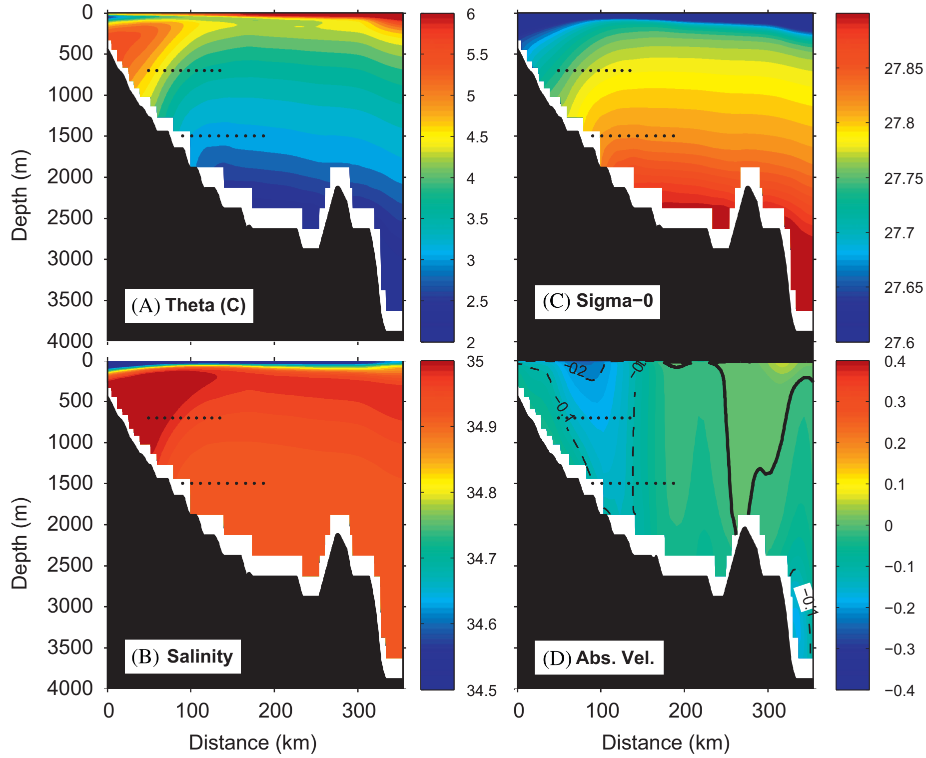

Fig. 6. The same as Fig. 3 but for mean FLAME model variables, 1987–2004. Small dots indicate e-float release sites in Experiment 1.

positions of the simulated trajectories in Experiment 1. The most noticeable difference compared to the observations from July 2003 (Fig. 3) is the much higher salinity at intermediate and deeper depths in the model, Fig. 6B. This is a known flaw in this and other North Atlantic general circulation models (Boening et al., 2003; Treguier et al., 2005), probably related to subtle errors/imbalances in the advective supply of freshwater to the convection regime of the central Labrador Sea (C. Böning, personal communication, 2010). Also, there is evidence of warm, salty Irminger Current water over the upper slope that is not evident in the observations. In the model mean velocity section (Fig. 6D), the DWBC is narrower, has slightly higher southward flow near the surface (>20 cm/s) and is more baroclinic (see isopycnal slopes in Fig. 6C). As with the RAFOS release sites, the model release sites are all embedded within the mean southward flow and extend well inshore of the velocity maximum. Thus it appears that both the RAFOS and the e-floats were released at sites spanning the width of the DWBC and were not biased toward its offshore edge.

To compare the observed and numerical trajectories as accurately as possible, we first selected 59 e-floats from the population of 5360 3D trajectories and plotted them on the same scale as Fig. 4A (Fig. 7A). These e-floats were randomly selected from the two float depths and multiple launch sites to obtain the same depth and cross-slope launch distribution as the RAFOS floats (see Fig. 2), that is with more of 700 m than 1500 m floats and more inshore than offshore floats. Changes in color along the e-float trajectories indicate float depth, and illustrate the deepening of the floats as they move away from the boundary and into the Newfoundland Basin and subtropical gyre where the isopycnals deepen.

The behavior of the 59 simulated two-year trajectories is similar to that of the RAFOS floats in that: (1) nearly all of the e-floats initially drift southward over the continental slope toward Flemish Cap, (2) a subset of 700 m e-floats drifts through Flemish Pass, (3) most of the e-floats detach from the boundary and drift into the interior east of the Grand Banks, forming a similar tangle of trajectories there, and (4) relatively fewer floats are exported south and west of the Grand Banks compared to those that are not exported (i.e., retained in the subpolar region). The e-float trajectories differ from the RAFOS float trajectories in that they do not drift as far east or south and a few drift farther north. From the displacement vectors (Fig. 7B) it is apparent that a lower fraction (17%) of e-floats was exported compared to the RAFOS floats (29%), again based on float positions two years after “release” at 50°N. The exported e-floats were also distributed somewhat differently among the three subgroups: only 2% (compared to 17% of RAFOS) ended up in the subtropical interior, 3% (compared to 7% of RAFOS) were in the DWBC and the remaining 12% (compared to 5% of RAFOS) were in the Slope Water.

A more statistically robust estimate of the spreading pathways of LSW in FLAME can be obtained by considering the whole population of e-floats released at 50°N. The destination statistics for the entire population of 5369 3D e-floats are summarized in Fig. 5B. Agreement with the RAFOS float destination statistics is better when the entire population is considered. The percentage of exported e-floats is 21% compared to 29% for RAFOS, and the percentage of e-floats exported to the subtropical interior is 7% versus 17% for RAFOS.

Are these differences significant? This is a difficult question to answer when there are only 59 RAFOS float displacement vectors. The model output offers the only option for estimating the variability in destination statistics for ensembles of 59 floats. The destination statistics for 100 ensembles of 59 e-floats each were calculated and the mean and standard deviation are illustrated in Fig. 5C. Again, each ensemble had a depth and cross-slope launch distribution matching the RAFOS floats. The percentage of exported RAFOS floats is larger than the mean of the 100 e-float ensembles by 1.4 standard deviations (29% for RAFOS versus $22\pm5\%$), but within the range in percentage of exported floats over the 100 ensembles, 10–34%. Five percent of the e-float ensembles had the same or higher fraction of floats exported as the RAFOS floats.

Considering next the subgroups within the exported floats, we find that again, more RAFOS floats were exported via the DWBC, but

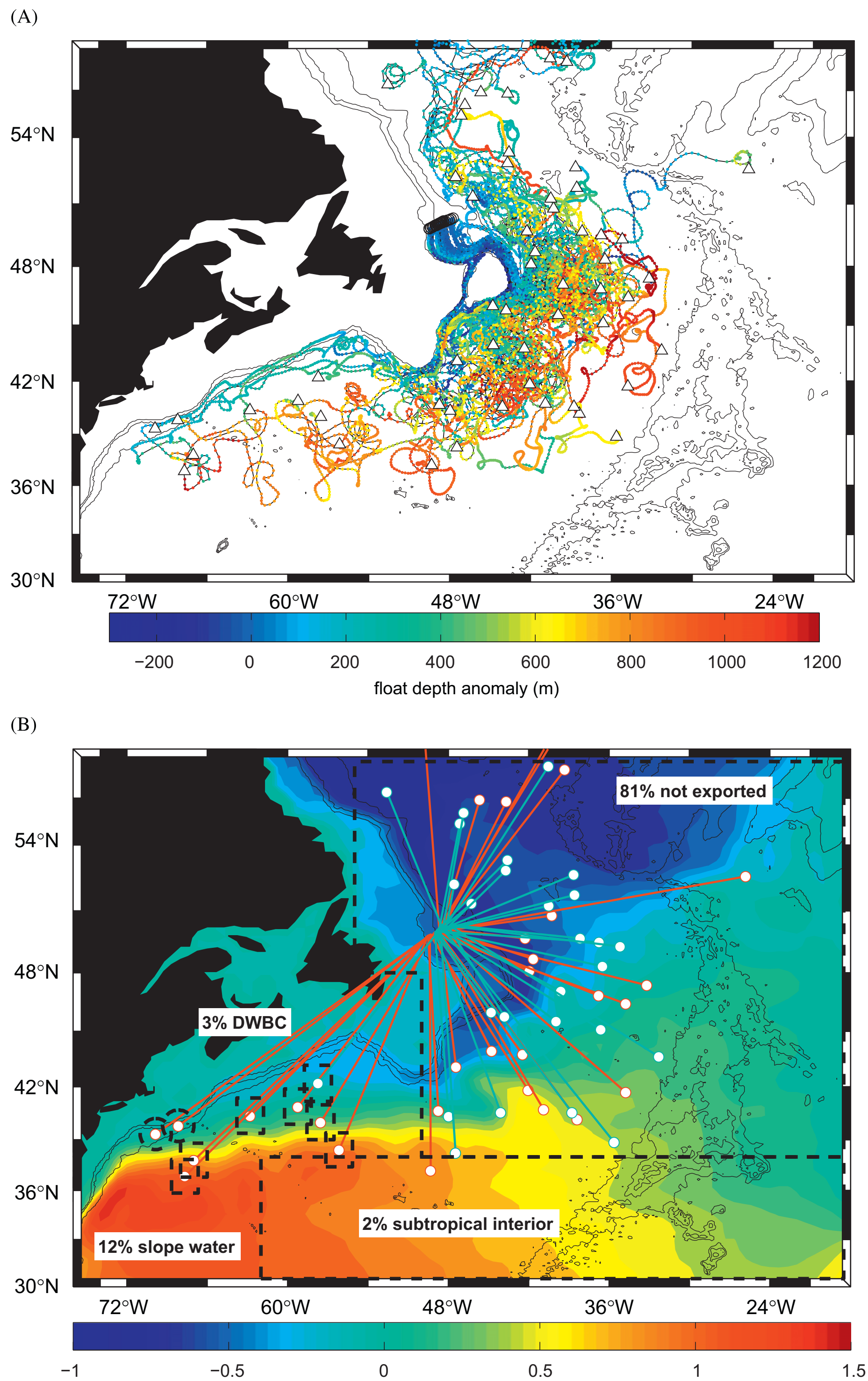

Fig. 7. (A) Two-year trajectories of 59 3D e-floats with the same depth and cross-slope launch site distribution as the RAFOS floats. Color indicates float depth along the trajectory. (B) Displacement vectors for trajectories in (A), color-coded by initial depth, 700 m (red) and 1500 m (blue), and superimposed on the mean streamfunction for the top layer of FLAME.

within one standard deviation of the model ensembles (7% RAFOS versus 5 ± 3%). The same cannot be said for the e-floats following the subtropical interior pathway: the model indicates only 7 ± 3% whereas the observations indicate 17%, or about three standard deviations higher. In 100 random ensembles of e-floats, there were no cases with 17% (10 floats) exported to the subtropical interior and only one ensemble with nine floats. Rather than exporting floats to the subtropical interior, the model exports a larger percentage on average to the Slope Water, 10 ± 3% compared to 5% in the RAFOS floats.

Possible explanations for these differences will be discussed in later sections, but here we provide a first piece of evidence that they are not due to the fact that the RAFOS floats are isobaric while the e-floats are isopycnal. The destination statistics for 100 sets of 59 2D trajectories are illustrated in Fig. 5D. Even *fewer* 2D e-floats are exported in this case (17% versus 22% for 3D and 29%

for RAFOS), suggesting that this is not an explanation for the data-model differences described above. Furthermore, the partitioning among the three exported subgroups is similar in the 2D and 3D e-float populations (e.g., subtropical interior floats make up 35% of 2D floats and 32% of 3D floats compared to 59% of RAFOS floats). So the differences in export to the subtropical gyre cannot be easily explained by the isopycnal–isobaric difference.

In summary, we showed here that the RAFOS floats were released across the entire width of the DWBC at 50°N, and thus should represent LSW pathways from inshore, center and offshore parts of the DWBC. Using the surface locations of the floats to determine how many were exported to the subtropics, we found that only 29% was exported in two years, with most of these (59%) following an interior pathway to the subtropical interior and only 24% following the DWBC path around the Grand Banks. Using 100 ensembles of simulated floats with the same depth and cross-slope distributions as the RAFOS floats to estimate the mean and variations in destination statistics for the model, we found that the model does a reasonably good job at reproducing the RAFOS float spreading pathways except that it underestimates the strength of the subtropical interior pathway. Repeating the analysis with 2D numerical floats did not significantly change this difference, an initial indicator that the subtropical interior pathway observed with the RAFOS floats is not an artifact of their being isobaric drifters. This topic will be revisited in Section 3.5.

3.4. *Dependence of float depth and release site on export*

Next, we consider whether float depth or release site influences the chances of a float being exported to the subtropics. Fig. 8A shows that 700 m RAFOS floats were somewhat more likely to be exported within two years compared to 1500 m floats (blue bars; 34% versus 22%). For comparison, we calculated the same statistics for the 100 groups of 59 3D e-floats with the same release distribution as the RAFOS floats (red bars; see Section 3.3). They show a stronger tendency for more 700 m e-floats to be exported compared to 1500 m floats. The percentages agree within one standard deviation for the 700 m floats, but the model significantly underestimates the number of 1500 m floats exported compared to RAFOS, perhaps because 1500 m e-floats released at the offshore sites were almost all recirculated (see below).

The RAFOS floats were released at several cross-slope locations to determine if LSW closest to the slope remained longer in the DWBC and followed a more direct path to the subtropics compared to those released farther offshore (see Fig. 3 for release sites). Fig. 8B shows a monotonic decrease in the percentage of floats exported with increase in distance offshore, with 35% of the site 1 (s1) floats exported and only 20% of the site 3 (s3) floats. The same trend is even more pronounced in the model trajectories. The model and data percentages match within about one standard deviation for the two inshore sites, but the model is apparently much less successful at exporting floats from the offshore site.

Examination of the individual RAFOS float trajectories revealed that nearly half (43%) of the 700 m floats released at the two inshore sites drifted through Flemish Pass, the 1100 m deep gap between the Flemish Cap and the Grand Banks (see Fig. 1A for location). This route appears to be an "inside track" that substantially increases the likelihood of a float being exported to the subtropics. This is illustrated in Fig. 8C, which shows that 700 dbar RAFOS floats that go through the Pass are about four times more likely to be exported than 700 dbar floats that go around Flemish Cap (recall that 1500 dbar floats are too deep to go through Flemish Pass and are therefore omitted from Fig. 8C). This considerable difference is also illustrated in Fig. 9, which shows the trajectories of 700 m RAFOS floats that went through

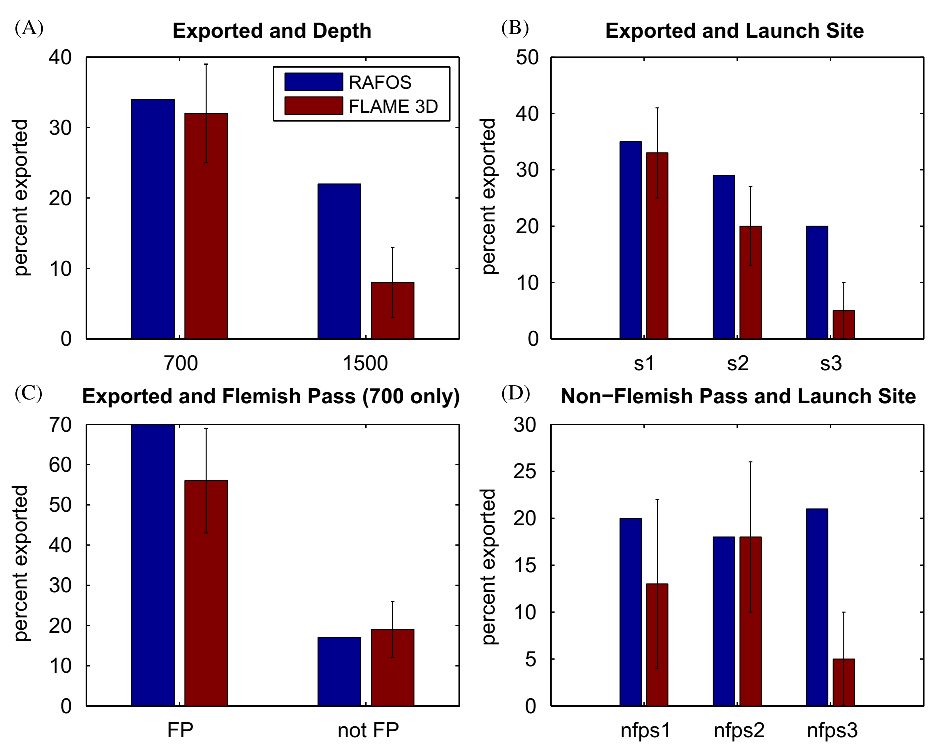

Fig. 8. Histograms showing the percentage of RAFOS and e-floats that ended up south and west of the Grand Banks in two years ("exported") as a function of (A) float depth, (B) launch site across the continental slope and (C) whether the float drifted through Flemish Pass. Red bars are for RAFOS; blue for 100 ensembles of 3D e-floats. Vertical bars on the latter indicate one standard deviation around the mean for the 100 ensembles.

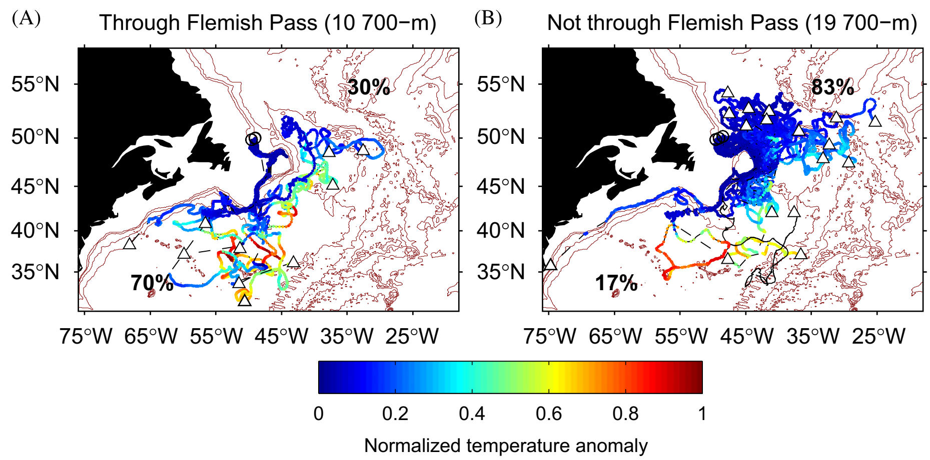

Fig. 9. (A) Trajectories of 10 700 m RAFOS floats that drifted through Flemish Pass. Seventy percent of these floats were exported. (B) Trajectories of 19 700 m floats that drifted around the seaward flank of Flemish Cap. Only 17% of these floats was exported.

the Pass (Fig. 9A) and those that did not (Fig. 9B). In general, the Flemish Pass floats drifted southward higher up on the continental slope and reached the Tail of the Grand Banks (TGB) before crossing the slope into deeper water. On the other hand, RAFOS floats that went around the Cap were expelled from the DWBC much farther north. The same trend is apparent in the e-float trajectories, Fig. 8C, and the percentages match the data within about one standard deviation.

These results point to Flemish Pass as an important conduit for lighter vintages of LSW to reach subtropical latitudes. From a hydrographic section across the Pass and the eastern flank of the Cap in August 1998, M. Rhein and colleagues measured elevated concentrations of chlorofluorocarbon (CFC-11) in the density range of Upper LSW (27.68–27.74 sigma-0; Kieke et al., 2006) in the Pass compared to the eastern flank of Flemish Cap (D. Kieke, personal communication, 2009). Observations of the currents in Flemish Pass are scarce due to the intense fishing activity there. Petrie and Buckley (1996) report on results from an array of current meter moorings that were deployed in the Pass for three months in 1985–1986 between the shelf-break and the 400 m isobath. Losses due to fishing reduced the data return to less than 50% of expected. Combining these observations with several other current meter studies, they showed that the southward flow associated with the Labrador Current is strongly sheared in the upper 400 m, then relatively uniform from 400 to 1000 m, ranging from 3 to 11 cm s^{-1} with a mean around 8 cm s^{-1}. The total volume transport through the Pass estimated from the compilation of observations was 6.3–9.8 Sv, a significant fraction of the 11.0 Sv reported for the combined baroclinic and barotropic Labrador Current by Lazier and Wright (1993) farther north off the Labrador coast. While there is significant uncertainty in the transport through the Pass, it is clear from Petrie and Buckley (1996) and references therein that the deep Pass (depths greater than 400 m) contains a southward flow that contributes significantly (65–80%) to the total transport through the Pass.

The observed and model trajectories clearly indicate that LSW that flows through Flemish Pass as opposed to around the seaward flank of Flemish Cap is more likely to be quickly exported south and west of the Grand Banks. Considering the elevated EKE levels immediately east of the Cap associated with the meanders and eddies of the NAC, it is not surprising that LSW flowing around the Cap will be more likely mixed into the interior than LSW that flows through the protected Flemish Pass. Furthermore, Fig. 8D shows that for the RAFOS floats that go around the Cap, their release site has little bearing on whether they are exported or not. This is also true for the model floats except that Cap floats released at the offshore site are much less likely to be exported. These results point toward the importance of Flemish Pass for monitoring the LSW that will be most quickly exported to the subtropics.

3.5. Isopycnal versus isobaric trajectories around the Grand Banks

In this section, we will address the third and final question raised in the introduction, namely was the dominance of the interior pathway into the subtropics compared to the DWBC pathway observed by B09 and reinforced in Section 3.2 of this paper an artifact of the isobaric constraint on float motion? Would the DWBC has been the dominant pathway if the RAFOS floats had been isopycnal? G06 argued that the answer to this question is "yes" based on an analysis of simulated e-float trajectories released at 43°N and calculated using the time-mean FLAME velocity field. B09 argued that the answer is "no" based on the fact that 3D and 2D e-floats released near 50°N and calculated using the *time-varying* model velocity fields escaped from the boundary current in equal numbers. Here we will attempt to reconcile the apparently contradictory results of G06 and B09 by closely replicating the numerical float experiment of G06 using both the time-mean and time-varying velocity fields to calculate simulated trajectories from the same location at 43°N, just upstream of the TGB. We will also show from the RAFOS observations that there is little evidence of vertical motion as the floats cross the continental slope out of the DWBC near the TGB, indicating that isopycnal and isobaric drifters at the LSW level would behave similarly in this region.

G06 argued that isobaric RAFOS floats would underestimate the transport of LSW rounding the TGB based on the differences between 3D and 2D model float trajectories calculated using a time-mean FLAME model velocity field. The mean used was from the last year of the model spin-up. They calculated trajectories (the same as streamlines for time-mean velocity field) of e-floats initialized at 43°N between 50 and 46°W at depths between 700 and 2000 m. In one calculation, they used the full three-dimensional mean velocity field to compute trajectories (3D), while in the other they used only the horizontal velocity components (2D). G06 then restricted their analysis to only those e-floats that crossed 32°N in the DWBC to focus attention on those fluid parcels that could be considered part of the AMOC. They found that in the 3D case, 58% of these floats rounded the TGB in the DWBC (defined as crossing both 50° and 55°W in the boundary current), while in the 2D case, only 41% followed this path, 30% less than for the 3D case. G06 explained this difference by pointing out that at the TGB, the zero in mean velocity (which separates the mean westward-flowing DWBC from the mean eastward-flowing GS) is displaced offshore with increase in depth, and that the shallower ''isobaric'' e-floats, unable to follow the downward sloping isopycnals, were turned back eastward along the path of the Gulf Stream (their Fig. 3).

Given the relatively large eddy variability in the vicinity of the TGB (see Figs. A3–A5), it seems important to consider the difference in spreading pathways of 3D and 2D e-floats released at 43°N using the time-dependent model velocity fields to determine if there would be a substantial difference in isopycnal or isobaric float trajectories. In Experiment 2 (see Section 2), we initialized more than 8000 e-floats at 43°N and used the model mean field for the years 1994–1998 in one case and the time-varying fields for those years, repeated in sequence, to calculate fifteen-year e-float trajectories. In each case, 2D and 3D e-float data sets were produced. From each run we analyzed only those e-floats that were released in the DWBC, defined as a southward drift over the first three days from release inshore of the 4000 m isobath (see Section 2 and Table 1 for summary of various runs). This approach was taken to focus on the 3D and 2D pathway differences for all the floats released in the DWBC at 43°N, not just the much smaller number that ultimately crossed 32°N in the DWBC, as was considered by G06.

Fig. 10A–D shows the spreading pattern of the 3004 3D e-floats initialized at 43°N in the DWBC after 12, 40, 120 and 365 days when the time-mean model velocity field is used to generate the trajectories. Colors indicate e-float depth at release. This figure is analogous to Fig. 3 in G06, and shows a similar pattern. Only two pathways emanate from the TGB: one along the continental slope in the DWBC and the other offshore along the path of the NAC (see Fig. A2 for mean model surface circulation). Twenty-seven percent of these e-floats followed the DWBC continuously around the TGB inshore of the 4000 m isobath to 55°W: these 802 e-floats are indicated by larger dots in Fig. 10A–D. Many dots are superimposed along the continental slope because the mean streamlines closely follow the topography at all depths seeded with e-floats.

Curiously, the 3D and 2D runs indicate about the same percentage of e-floats following the DWBC path: 27% for 3D and 25% for 2D (Table 2). This contradicts the results of G06, who found a 30% difference in the fraction of 2D and 3D e-floats following the DWBC path around the TGB. We speculate that the difference is due to the use of only one model year for the mean field.

The same plots but using the time-dependent model velocity fields are shown in Fig. 10E–H. The impact of eddies on LSW spreading is immediately obvious from the expanding cloud of e-float locations with time. Some e-floats follow the DWBC inshore of the 4000 m isobath to 55°W (larger dots), but these make up only 3% of the 3646 e-floats released in the DWBC, an order of magnitude less than for the case using the mean velocity (Tables 2 and 3). The e-floats spread more or less uniformly east and south of the Grand Banks, many reaching the subtropical interior (defined previously as south of 38°N) within one year. As in the case using the mean velocity field, the difference between 3D and 2D is not significant—5% of the 2D versus 3% of the 3D e-floats follow the DWBC continuously around the TGB (Table 3).

From these model results, we conclude that at least in FLAME, there is little difference in the ability of 3D and 2D e-floats to follow the DWBC path continuously around the TGB from 43°N to 55°W. This indicates that LSW is lost from the DWBC over the continental slope by some process that does not involve significant vertical motion along isopycnals. Another important point, somewhat understated by G06 but emphasized here is that when the more realistic time-dependent velocity fields are used to determine the pathways of floats released in the DWBC, vastly more particles are lost from the DWBC around the TGB. For both 2D and 3D, only a very small fraction negotiates this path ($\sim$5%), while the great majority are swept offshore at the TGB.

Returning to the RAFOS float observations, we can use the temperature records along the float trajectories to test whether they were diverted away from the DWBC around the TGB because of their inability to follow the vertical displacements of fluid parcels. Shaw and Rossby (1984) showed that for purely horizontal motion, isobaric floats will observe little change in temperature (Fig. 11A), whereas if there is a vertical component to the motion, isobaric floats will record an increase (for downward motion) or decrease (for upward motion) (Fig. 11B). They used this fact to argue that isobaric SOFAR floats crossing the Gulf Stream were indicating vertical motions along sloping isopycnals. Bower and Hunt (2000a; 2000b) also exploited this fact to show that increase in temperature along the trajectories of isobaric RAFOS floats advected southward by the DWBC near Cape Hatteras was evidence of deep waters flowing downward across the continental slope in order to cross under the Gulf Stream and preserve its potential vorticity. The same situation might be expected at the TGB when the Gulf Stream meanders over the continental slope. Based on the conceptual model of Shaw and Rossby (1984), if there is little change in temperature observed by an isobaric RAFOS float as it crosses the continental slope out of the DWBC, we can infer that there is little vertical motion and that isobaric and isopycnal drifters' trajectories would be similar.

Fig. 12 shows an example of a RAFOS float that maintained near-constant temperature as it crossed the continental slope at the TGB. Shown are bi-weekly images of total dynamic height from AVISO (combination of sea surface height anomaly with a map of mean dynamic topography Rio05, derived from GRACE, surface drifters, hydrography and altimetry; Rio and Hernandez, 2004) with float trajectory segments for float #673 (highlighted) and all other floats in the area at the same time. The dynamic topography is useful for identifying mesoscale eddies and the Gulf Stream front, but note that the smoothing inherent in the objective mapping removes submesoscale features. On 1 March 2006, float #673 was just inshore of the 2000 m isobath, measuring a temperature of 3.4 °C (Fig. 14B), as it began to drift around the southern tip of the Grand Banks. During the next 28 days, this 1500 m float crossed nearly the entire width of the slope, crossing the 4000 m isobath by 29 March 2006. During this crossing of the slope, the float drifted mainly parallel to the height contours, which indicate a surface geostrophic current that also crosses the topography. Temperature remained constant within about 0.2 °C during the crossing, a small temperature change compared to the >1 °C temperature increase that the float experiences later when it crosses the Gulf Stream. There was at least one cusp and one anticyclonic closed loop in the trajectory as the float crossed the slope, possibly indicating the formation of an anticyclonic eddy at the TGB (see below).

The float continued to drift southward during April 2006, approximately parallel to the surface flow. During the first half of May 2006, when the float was well south of the continental slope, the float accelerated and temperature began to increase significantly (Fig. 14B) as it crossed through the complex eddy field associated with the Gulf Stream. The RAFOS float meandered around this general area for the next year, measuring temperatures between 4.0 and 4.7 °C, eventually surfacing at 36°N two years after release (not shown).

The temperature increase observed by this float where it met the Gulf Stream is an indication of subduction along isopycnals (Shaw and Rossby, 1984). At this point, the isobaric nature of the RAFOS float constrains its ability to follow a fluid parcel, and the two will separate. However, even though the two trajectories diverge at this point, we expect both are similarly affected by the

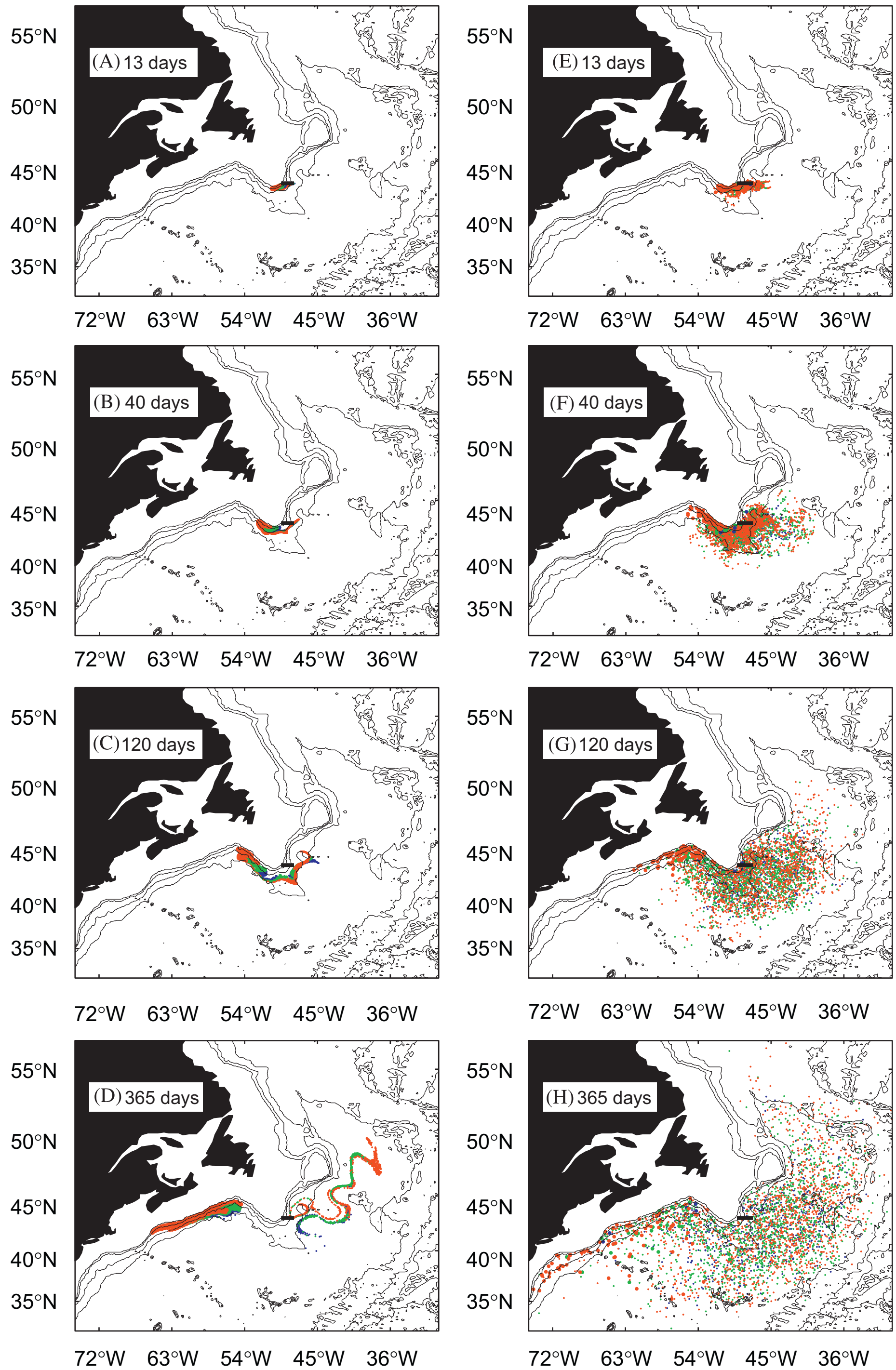

Fig. 10. (A–D) Positions of 3004 3D e-floats 13, 40, 120 and 365 days after release at 43°N when the 1994–1998 mean model velocity field is used. Color indicates float depth at release: 700–1000 m (red; 1290 e-floats), 1000–1500 m (green; 1199 e-floats) and 1500–2000 m (blue; 515 e-floats). There is significant over-plotting as the e-float trajectories at different depths are very similar. Larger dots denote those floats that drifted continuously along the DWBC to 55°W. (E–H) The same as (A–D) but using the 1994–1998 time-dependent velocity fields to calculate the e-float trajectories. In this case, there are 1496 e-floats released at depths 700–1000 m, 1530 e-floats between 1000 and 1500 m and 620 between 1500 and 2000 m. The 1000, 2000, 3000 and 4000 m isobaths are drawn.

Table 2
Numbers of 3D and 2D e-floats released at 43°N, which are advected around the TGB inshore of the 4000 m isobath that drift initially southward after release at 43°N using the 1994–1998 time-mean model velocity field.

	3D	2D
Total released (43°N, 50–46°W, 700–2000 m)	8317	8317
Released inshore of 4000 m isobath and drift initially southward	3004	3001
Cross 55°W in DWBC (i.e., without crossing 4000 m isobaths)	802 (27% of 3004)	765 (25% of 3001)

Table 3
The same as Table 2 but for e-float trajectories calculated using the 1994–1998 time-dependent velocity fields.

	3D	2D
Total released (43°N, 50–46°W, 700–2000 m)	8360	8360
Released inshore of 4000 m isobath and drift initially southward	3646	3630
Cross 55°W in DWBC (i.e., without crossing 4000 m isobaths)	119 (3% of 3646)	163 (5% of 3630)

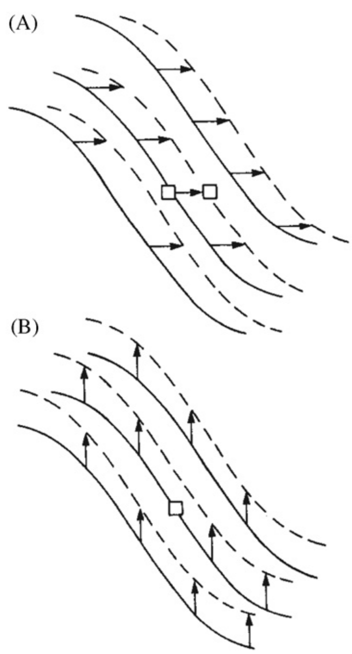

Fig. 11. Schematic showing the displacement of isotherms (curved lines) and an isobaric drifter (squares) in (A) a purely horizontal flow and (B) a purely vertical flow.
(From Shaw and Rossby, 1984).

high EKE in this region compared to the mean flow (Figs. A1, A3 and A4). Several studies have shown that at these depths, there is no potential vorticity gradient across the Gulf Stream and fluid parcels mix freely across it (Bower et al., 1985; Bower and Lozier, 1994). The main point here is that the separation of the float from the continental slope was not accompanied by a large temperature increase, suggesting that an isobaric RAFOS float trajectory is a good approximation to fluid parcel motion here. In other words, there is no evidence that the fluid parcel originally in the DWBC at 1500 m would have followed the DWBC around the TGB while the RAFOS float crossed the topography into deep water. Once offshore, we suggest that the vigorous eddy field will lead to spreading of LSW outward, including southward into the subtropical region.

The second example clearly illustrates the formation of an anticyclonic eddy at the TGB. Float #582, a 700 m float, was approaching the TGB over the upper continental slope (1000–1500 m water depth) on 16 August 2006 (Fig. 13A), measuring a temperature of about 3.8 °C (Fig. 14A). Again, the trajectory is mainly parallel to the surface geostrophic flow over the upper slope. Beginning in the first half of September 2006, it shot across the continental slope while maintaining a constant temperature within 0.1 °C. What begins as a few cusps in the trajectory turn into a series of closed anticyclonic loops with period 4–5 days and looping radius ~25 km by 1 October 2006. Two other 700 m floats began looping in the same feature (Fig. 13D). Temperature for 582 remained constant within about 0.2 °C during the looping, which continued for three months. The apparent eddy drifted slowly westward during this period, and the sea surface height indicates anticyclonic circulation at the surface, although a closed sea surface high is not always apparent. Looping ended abruptly around 3 January 2007 (Fig. 13E), the float accelerated southward and temperature increased in two steps to nearly 9 °C by 1 March 2007 (Fig. 13F–H and Fig. 14A), a clear indication that the eddy and the float were absorbed into the Gulf Stream. Eventually float 582 crossed the Gulf Stream and surfaced near 37°N, 48°W, placing it in the subtropical interior group.

This is one of several similar events in the RAFOS float data set where a coherent anticyclonic eddy apparently forms at the TGB and spins off some LSW from the boundary current. These eddies may have important implications for LSW spreading. Elliott and Sanford (1986a; 1986b) observed a lens of LSW in the subtropical gyre and speculated that it may have formed near the TGB. These eddies will be the subject of future work.

4. Discussion and summary

Inspired by earlier profiling float observations that showed no evidence of a continuous export of LSW from the subpolar North Atlantic along the continental slope around the Grand Banks, a new Lagrangian study of LSW export pathways was undertaken in 2003–2008 using acoustically tracked RAFOS floats. Here we analyzed results from the 59 isobaric floats, about half at 700 m and half at 1500 m, which were sequentially released in the DWBC at 50°N and tracked for two years. The main spreading pathways revealed by these floats reinforce the results reported by B09, which were based on only two-thirds of the final float data set. Specifically,

- Most (~70%) of LSW exiting the Labrador Sea at 50°N in the DWBC leaves the slope and recirculates within the ocean interior between 50 and 43°N. Only ~30% of the LSW is exported beyond the Tail of the Grand Banks within two years.
- In spite of preconceptions about the importance of the DWBC for transporting LSW to the subtropics, less than 10% of LSW is exported continuously along this path within two years.
- More LSW (~15–20%) is exported to the subtropics in two years via an interior pathway southward from the TGB.

The recirculation of most of the RAFOS floats within the subpolar region is somewhat consistent with the earlier profiling float results. In those studies, all of the floats exiting the Labrador Sea in the DWBC left the continental slope before reaching 43°N and drifted eastward at the subpolar–subtropical gyre boundary. In light of the fact that less than 10% of the RAFOS floats followed the DWBC path continuously around the Grand Banks, and the relatively smaller number of profiling floats, perhaps it is not surprising after all that none of the profiling floats rounded the Grand Banks in the DWBC. Over the continental slope (offshore of the baroclinic Labrador Current at the shelf-break), the southward flow of the DWBC is very barotropic (Fig. 3D), so profiling float displacements probably provide a good approximation to the flow at depth. However, once entrained into the baroclinic Gulf Stream or NAC, profiling floats will be strongly influenced by the surface-intensified currents during profiling and their ability to follow deep fluid parcel trajectories will deteriorate, as also

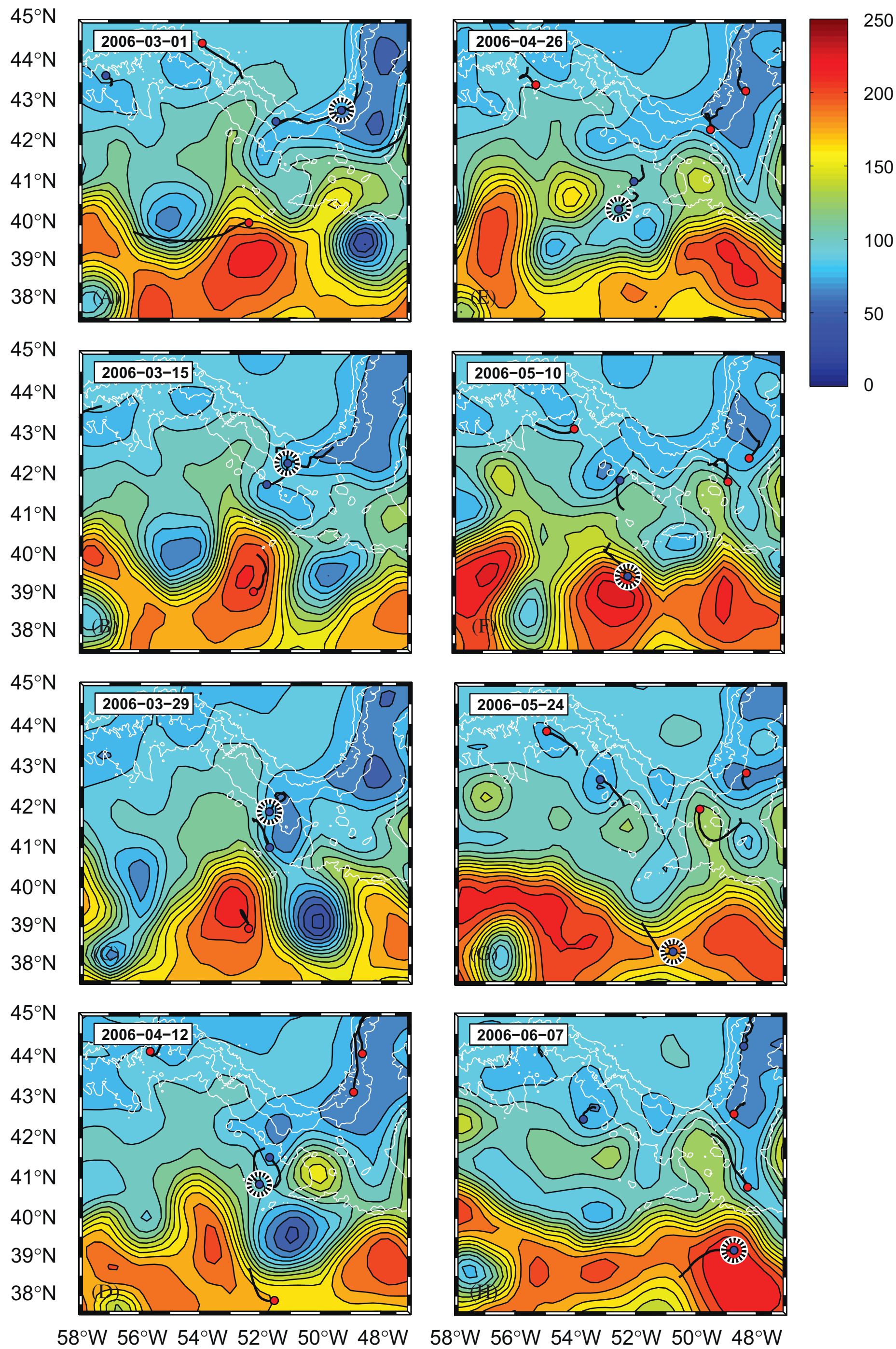

Fig. 12. Bi-weekly images of total dynamic topography from Aviso with 12-day RAFOS float trajectories for the time period 1 March–7 June 2006. Colored circle indicates segment head, blue for 1500 m floats and red for 700 m floats. Float #673 is highlighted in each panel.

pointed out by G06 in the context of FLAME. This could explain why the subtropical interior pathway was never sampled by the profiling floats: they would be displaced downstream on every surfacing.

The large offshore export of both float types east of the Grand Banks is also consistent with the along-boundary decrease in LSW transport observed with direct velocity measurements. Dengler et al. (2006) report a mean LSW (sigma-0 = 27.68–27.80) transport at 56°N of -17.2 ± 3.4 Sv during 1996–2005 from seven repeated combined shipboard ADCP/LADCP sections. Schott et al. (2006) obtained a mean transport of only 7.0 Sv in the same density layer at 43°N based on four sections occupied between 1999 and 2005. This $>50\%$ loss of LSW transport between 56° and 43°N is qualitatively similar to the $\sim 70\%$ loss of RAFOS floats from the DWBC between 50 and 43°N. The RAFOS floats further point to the southeastern corner of Flemish Cap as the primary location of offshore recirculation. The fact that most of the recirculated RAFOS floats did not become re-entrained into the DWBC within two years is an indication that this is a true recirculation and not just a local exchange of fluid parcels between the DWBC and the interior, although some local detrainment and re-entrainment were also observed.

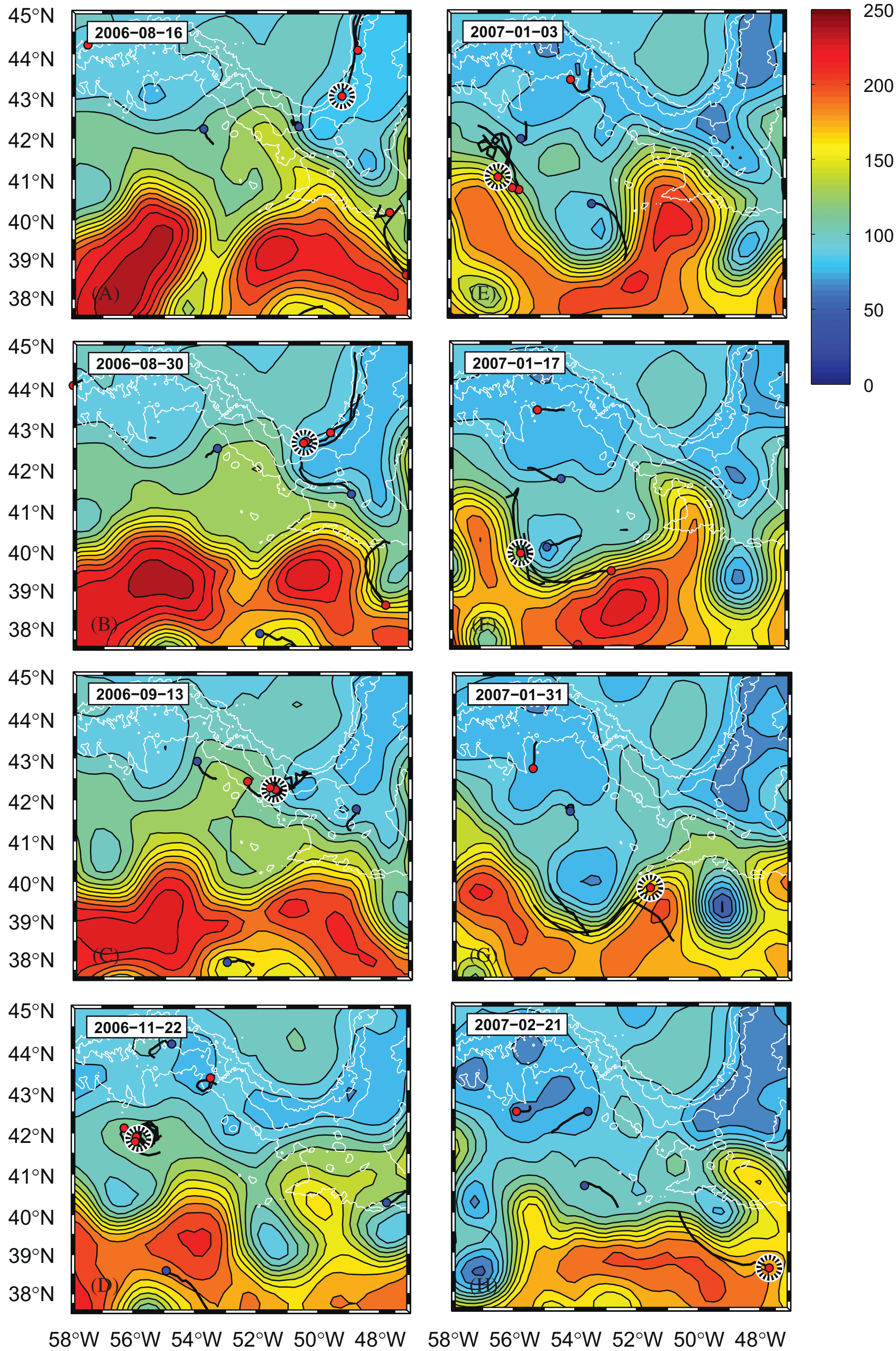

Fig. 13. The same as Fig. 12 but for the time period 16 August 2006–21 February 2007. Float #582 is highlighted. Note that the time interval between images is not constant.

In B09, it was shown that the spreading pathways of LSW revealed by thousands of numerical trajectories calculated using velocity fields from the high-resolution (1/12°) general circulation model FLAME were qualitatively similar to the RAFOS floats. Here we took the analysis of the Lagrangian characteristics of FLAME a step further by comparing the positions of observed and model floats with the same release distribution two years after release at 50°N. Agreement was generally good. Specifically, it was found that

- As with the observations, most (78 ± 5%) of the e-floats recirculated offshore before reaching the TGB, and < 10% (5 ± 3%) followed the DWBC pathway continuously around the Grand Banks.
- The most significant differences were that more model floats initialized at the outer edge of the DWBC were recirculated compared to the observations, and that the model under-estimated the percentage of e-floats exported to the subtropics via the interior pathway compared to the RAFOS floats, sending more e-floats into the Slope Water region instead. In 100 ensembles of 59 3D (or 2D) e-floats, the average number following the interior pathway was less than half that for the RAFOS floats, 7 ± 3% (6 ± 3% for 2D), and none had as

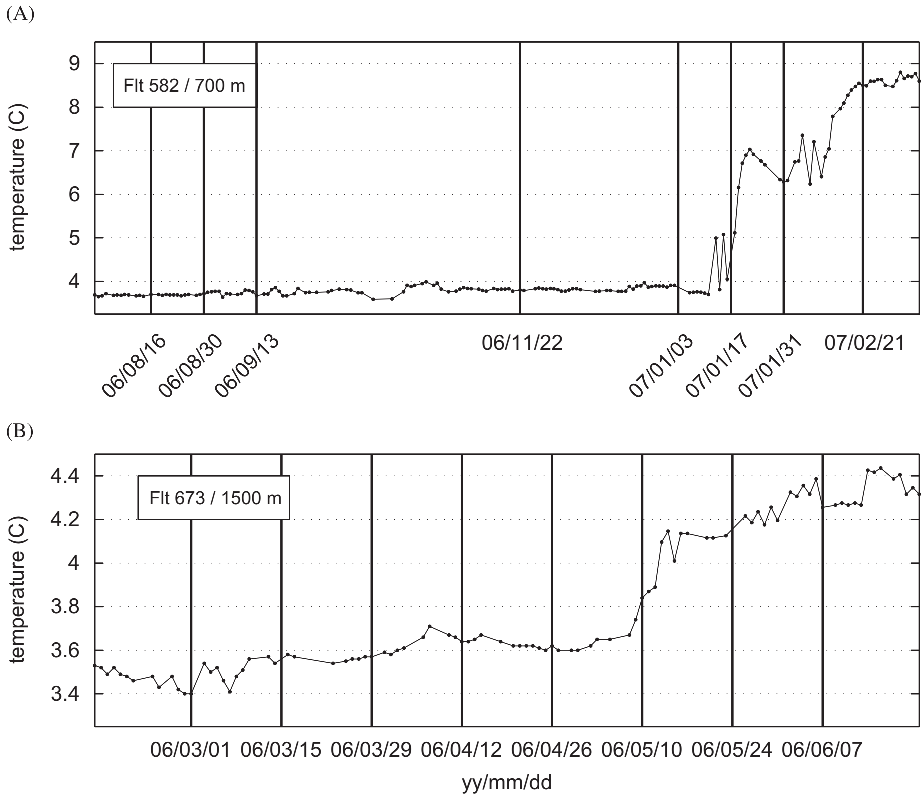

Fig. 14. Temperature measured by (A) float #582 and (B) float #673 during the time periods represented in Figs. 13 and 12, respectively. Vertical lines correspond to the dates of the individual images.

many as 10 e-floats ending up in the subtropical interior after two years.

With only 59 RAFOS floats, it is impossible to determine if this difference is because the ensemble of RAFOS float pathways is a statistical outlier, or the model is somehow deficient in its ability to more closely reproduce the RAFOS float results. We can however point to one aspect where the Eulerian characteristics of FLAME differ from observations in a way that could explain the differences in Lagrangian behavior. As shown in the Appendix, the model appears to underestimate EKE in the Gulf Stream region south and west of the Grand Banks, and perhaps overestimate the same east of the Grand Banks, at least at the sea surface. If this pattern extends to the depth of LSW, it could explain the extra dispersion of model floats eastward and the lower number of model floats exported to the subtropical interior, the argument being that dispersion of fluid parcels is proportional to EKE.

More detailed analysis of the RAFOS and model float trajectories and related observations revealed that

- The floats were released at sites that span the width of the tracer and velocity signatures of the DWBC at 50°N, indicating that their trajectories should be representative of the spreading of LSW from the inner as well as outer parts of the DWBC.
- Flemish Pass, the 1100 m deep channel between the Flemish Cap and the Grand Banks is an important shortcut for LSW with sigma-0 < 27.76 kg m^{-3} near the continental slope to be more rapidly exported to subtropical latitudes. Fifty-percent more 700 m RAFOS floats were exported to the subtropics in two years compared to the 1500 m floats (34% versus 22%) because of this protected pathway.

One of the most striking results of B09, reinforced here with the full RAFOS float data set from the Export Pathways project, was the large number of floats that drifted southward into the subtropical interior from the vicinity of the TGB compared to the number that followed the DWBC continuously around the Grand Banks. Two arguments were presented here to show that this result is not an artifact of the RAFOS floats being isobaric and not isopycnal drifters.

- The RAFOS floats measured relatively cold and constant temperatures as they crossed the continental slope into deep water at the TGB, indicating that there is little vertical motion associated with the detachment and that isopycnal and isobaric drifters would behave similarly. Evidence was presented using contemporaneous sea surface height fields that LSW is peeled off the continental slope by eddies at the TGB.
- Following the approach of G06 but using the time-varying FLAME velocity fields to calculate thousands of numerical float trajectories around the TGB rather than the time-mean, it was shown that isopycnal and isobaric floats are equally likely to follow the DWBC continuously around the TGB.

In closing, we raise an important question that remains unanswered, namely what is the relevance of the results presented here to the equatorward spreading pathways of the deeper, denser components of NADW, Denmark Strait Overflow Water and Iceland-Scotland Overflow Water. We have shown here that the spreading pathways of the intermediate-depth LSW are directly influenced by the eddy field associated with the Gulf Stream and NAC where it impinges on the continental slope around the Grand Banks. It has been shown with historical hydrographic observations and numerical models that the eddies also have an *indirect* impact on LSW spreading pathways, driving mean recirculation cells that transport LSW to subtropical latitudes (Lozier, 1997; Gary et al., 2011). The mean Gulf Stream and NAC have been shown to extend to the sea floor in this region and the high EKE associated with their meanders and eddies also extends to the bottom (Schott et al., 2006; Hogg, 1992; Bower and Hogg, 1996), providing a mechanism for the stirring of overflow waters from the slope into the ocean interior. There is also evidence that the mean recirculations extend to the depth of the overflow waters (Lozier et al., 1995). On the other hand, the constraint imposed on the overflow waters by the sloping topography is likely stronger, and they may be more inclined to follow the DWBC pathway around the Grand Banks. New observational and modeling studies are being planned to pursue this question. The answer bears strongly on the connectivity of the deep limb of the AMOC and on the response of the ocean to climate change.

Acknowledgments

We thank E. Colbourne and his team from the Northwest Atlantic Fisheries Centre in St. John's, Newfoundland, for their long-term commitment to deploying most of the RAFOS floats used in this study. Without their help, this field program would not have been possible. We are also grateful to WHOI engineers, J. Valdes and B. Guest, for their expert preparation of the RAFOS floats and sound sources, the captain and crew of the R/V *Oceanus* for their assistance in the deployment of the sound sources and first RAFOS float setting, and H. Furey for processing the RAFOS float data and helping with final figure preparation. J. Fischer of IFM-GEOMAR generously provided ship time for emergency replacement of sound sources. We also thank C. Böning for introducing us to the FLAME model, supporting one of us (S. Gary) in transferring the numerical float code to Duke University, and generously sharing his expertise of FLAME and other North Atlantic models. This work has also benefited from discussions with T. Rossby, K. Getzlaff, J. Toole, D. Kieke, M. Rhein, M. McCartney, D. Amrhein and J. Fischer. The research was supported by the US National Science Foundation.

Appendix. Mean circulation and eddy kinetic energy at the sea surface around the Grand Banks: model-data comparison

A1. Mean surface circulation

We compare the mean velocity field from a near-surface layer (49 m; layer 5) of FLAME to that from the most recent combined mean dynamic topography (CMDT) from AVISO, called **MDT_CNES-CLS-09** (see http://www.aviso.oceanobs.com/en/data/products/auxiliary-products/mdt/index.html for methodology and improvements over previous product). The latter has a spatial resolution of 0.25° and applies to the time period 1993–1999. For consistency, we used FLAME output for the same years to construct the model mean.

The area of interest here is around the Grand Banks (35–54°N, 60–35°W). Fig. A1 shows the mean surface geostrophic velocity (vectors) and mean speed (color shading) from MDT09 ("observations"). Speed is contoured at the resolution of the MDT09 while only every other vector is plotted. Bathymetric contours are 1000:1000:4000 m (the model bathymetry is what is drawn here). Fig. A2 shows the same but for layer five of FLAME ("model") (with only every 6th vector plotted).

Both the model and observations show an eastward-flowing Gulf Stream entering the Grand Banks region from the west. At 60°W, the observations show a stronger mean eastward jet (peak mean speed 50–60 cm/s) centered at about 39.5°N compared to the model (peak mean speed 20–25 cm/s centered farther south at about 38.5°N). Both the observations and the model exhibit

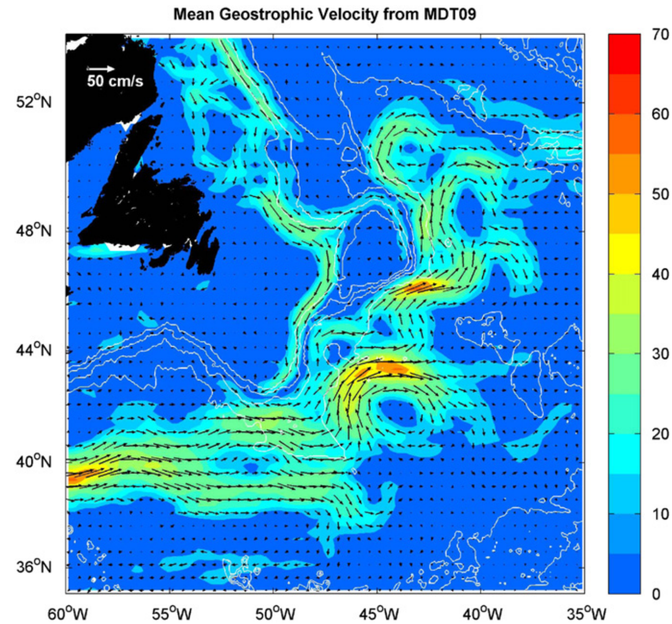

Fig. A1. Mean speed (color shading) and velocity (vectors) at the surface from the latest absolute mean dynamic topography product from AVISO. Only every other vector is plotted.

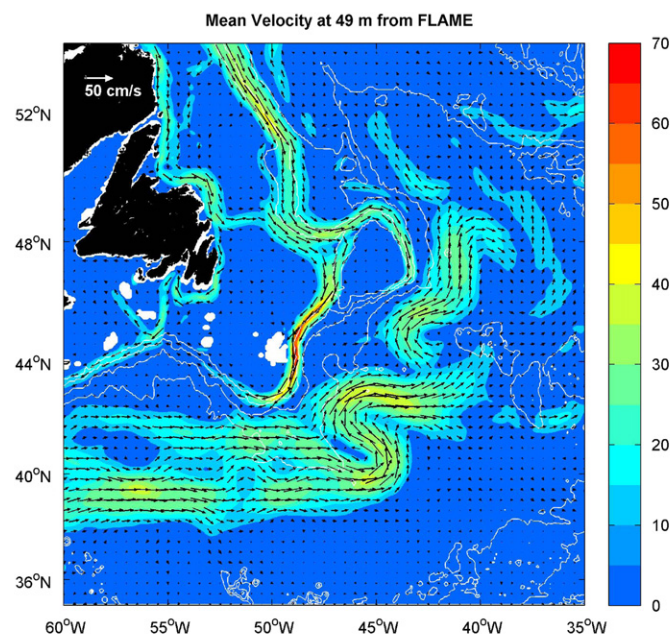

Fig. A2. The same as for Fig. A1 but for layer 5 of FLAME (49 m). Only every 6th vector is plotted.

some branching between 55° and 50°W: this is most clear in the observations, where one branch turns northeastward toward the Tail of the Grand Banks (TGB) and the other dips slightly toward the southeast. Both maps exhibit a similar convoluted path over the Southeast Newfoundland ridge (SENR), although the observations show mean flow approximately around the ridge in a southeastward trough, while the model indicates a more distinct, deeper and stronger trough displaced east of the ridge axis.

A clear anticyclonic Mann Eddy shows up in both maps, although in FLAME the eddy appears more like an anticyclonic meander than a closed circulation. Some of the highest mean speeds in the region are found on its northwest flank. The quasi-stationary sinuous path of the North Atlantic Current north of the SENR, previously reported by Rossby (1996), is clearly present in both model and observations, as is the brushing of the NAC against the southeastern corner of Flemish Cap (especially in the observations). A striking difference is apparent east of Flemish Cap, where the model indicates a well-defined retroflection of the NAC at about 48°N, whereas the observations indicate a mean northward flow farther inshore (over the 4000 m isobath) that continues to about 51°N, the so-called "Northwest Corner" (Worthington, 1976). It appears as if the eastward deflection of the NAC occurs about 2° latitude too far south in the model.

Turning to the Labrador Current (LC) that is evident flowing southward over the continental slope, the model indicates a much stronger LC. Peak mean speeds in the model reach 50–70 cm/s between Flemish Pass and the TGB, whereas the observations indicate peak speeds of only 25–40 cm/s. Both maps show strong LC flow through Flemish Pass; however, east of Flemish Cap, the model shows a strong LC whereas there is much weaker southward mean flow in the observations. The model may produce an LC that is too surface-intensified (C. Böning, personal communication), and/or the LC may be somewhat underestimated in the observations due to the spatial scale of the gridded altimetric product compared to the width of the LC. In both the model and observations, the LC mostly disappears in the mean west of the TGB.

The last feature of note here is that the observations indicate a westward recirculating flow of about 5–10 cm/s south of the Gulf Stream and west of about 45°W that is not well-reproduced in the model, where there is very weak mean flow.

A2. Eddy kinetic energy

To evaluate the distribution of eddy kinetic energy (EKE) in FLAME, we compare it to two EKE products derived from observations. The first is estimated from the altimetric-derived geostrophic velocity anomalies obtained from multiple satellites and mapped by AVISO on a 1/3° grid, Fig. A3. The second is based on the collection of all surface drifters deployed in the North Atlantic during the 1990s, binned into 1° boxes and analyzed by Fratantoni (2001), Fig. A4. It is expected that these two products provide lower and upper limits for comparison with the model EKE. Altimetric-derived EKE is likely biased low because of the wide ground track separation compared to the dominant eddy scales and the smoothing inherent in the objective mapping of the along-track measurements. On the other hand, drifter-derived EKE may be biased high due to currents driven by local wind variability, although Ducet et al. (1999) showed that this results in only a 20 $cm^2\,s^{-2}$ or less difference in EKE over the entire North Atlantic (see Fratantoni (2001) for detailed discussion of drifter and altimetric EKE differences). The altimetric and model (Fig. A5) EKE distributions are for the years 1993–1999 while the drifter map is for all of the 1990s.

Maximum EKE levels at the Gulf Stream axis where it enters the region from the west are similar in the altimetric observations and model, with peak values of just over 2000 $cm^2\,s^{-2}$. Maximum

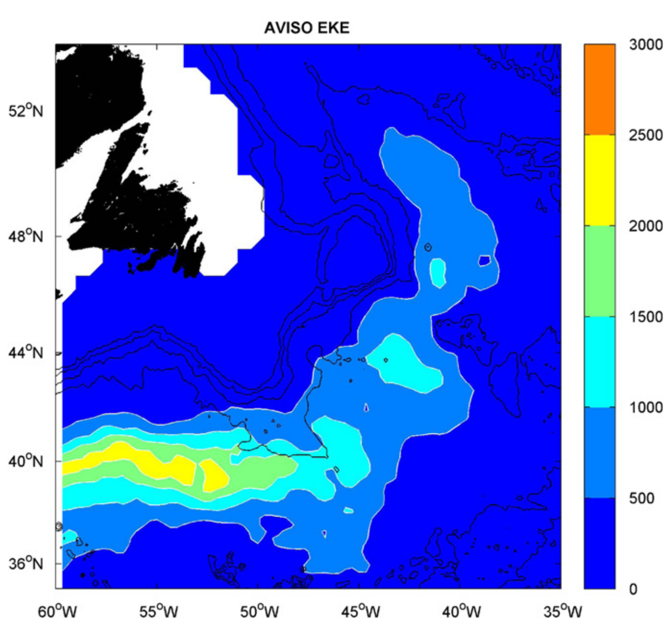

Fig. A3. Mean eddy kinetic energy from sea level anomalies. Contour interval is 500 $cm^2\,s^{-2}$.

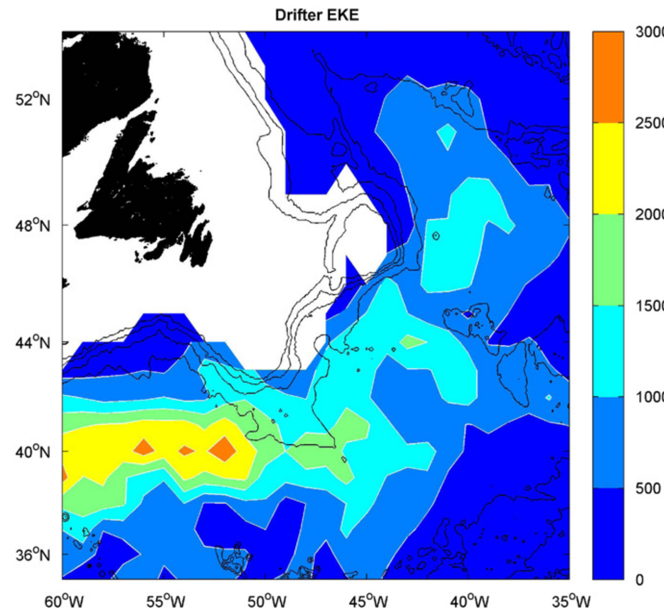

Fig. A4. The same as Fig. A3 but for the compilation of surface drifters released in the North Atlantic during the 1990s.
(Data courtesy of D. Fratantoni).

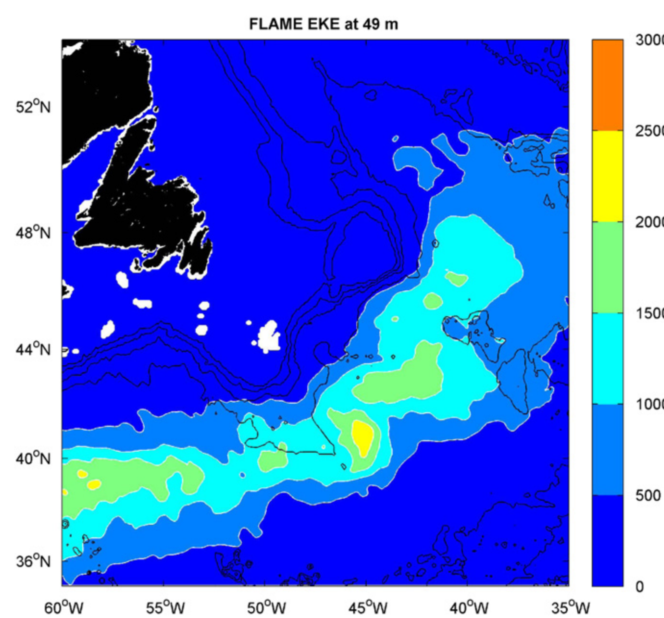

Fig. A5. The same as Fig. A3 but showing EKE from layer 5 in FLAME (49 m).

values are about 500 $cm^2 s^{-2}$ higher in the drifter EKE, as also pointed out by Fratantoni (2001). The high EKE ridge extends farther east toward the Southeast Newfoundland Ridge in the observations compared to the model. Like in the mean surface current, the axis of maximum EKE is offset to the south by about 1° latitude in the model. East of the Grand Banks and Flemish Cap, the model EKE overestimates the observed by about 500–1000 $cm^2 s^{-2}$. EKE values in the model are >1000 over a large area and reach a maximum of 1500–2000 $cm^2 s^{-2}$. In the altimetry, there are two smaller patches >1000 and the peak is only 1250 $cm^2 s^{-2}$.

Based on this cursory comparison, FLAME seems to reproduce fairly well the locations of most of the mean surface circulation features in the vicinity of the Grand Banks. The most significant differences are

- a mean and variable Gulf Stream that is too weak in the model between 60°W and the SENR;
- EKE values east of the Grand Banks, which are too high in the model;
- a Mann Eddy that is not closed in the model;
- a premature retroflection of the NAC in the model; and
- an LC that is too strong (at least at the surface) in the model.

References

Boening, C.W., Scheinert, M., Dengg, J., Biastoch, A., Funk, A., 2006. Decadal variability of subpolar gyre transport and its reverberation in the North Atlantic overturning. Geophys. Res. Lett. 33, L21S01. doi:10.1029/2006GL026906.

Boening, C., Rhein, M., Dengg, J., Dorow, C., 2003. Modeling CFC inventories and formation rates of Labrador Sea Water. Geophys. Res. Lett. 30. doi:10.1029/2002GL014855.

Bower, A.S., Hogg, N.G., 1996. Structure of the Gulf Stream and its recirculations at 55°W. J. Phys. Oceanogr. 26, 1002–1022.

Bower, A.S., Hunt, H.D., 2000a. Lagrangian observations of the deep western boundary current in the North Atlantic Ocean. Part I: large-scale pathways and spreading rates. J. Phys. Oceanogr. 30, 764–783.

Bower, A.S., Hunt, H.D., 2000b. Lagrangian observations of the deep western boundary current in the North Atlantic Ocean. Part II: the Gulf Stream-deep western boundary current crossover. J. Phys. Oceanogr. 30, 784–804.

Bower, A.S., Lozier, M.S., 1994. A closer look at particle exchange in the Gulf Stream. J. Phys. Oceanogr. 24, 1399–1418.

Bower, A.S., Rossby, H.T., Lillibridge, J.L., 1985. The Gulf Stream—Barrier or Blender? J. Phys. Oceanogr. 15, 24–32.

Bower, A.S., Lozier, M.S., Gary, S.F., Boning, C.W., 2009. Interior pathways of the North Atlantic meridional overturning circulation. Nature 459, 247.

Broecker, W.S., 1991. The great ocean conveyor. Oceanography 4, 79.

Bryden, H.L., Johns, W.E., Saunders, P.M., 2005. Deep western boundary current east of Abaco: mean structure and transport. J. Mar. Res. 63, 35.

Carr, M.E., Rossby, H.T., 2001. Pathways of the North Atlantic Current from surface drifters and subsurface floats. J. Geophys. Res. 106, 4405–4419.

Cunningham, S.A., Kanzow, T., Rayner, D., Baringer, M.O., Johns, W.E., Marotzke, J., Longworth, H.R., Grant, E.M., Hirschi, J.J., Beal, L.M., Meinen, C.S., Bryden, H.L., 2007. Temporal variability of the Atlantic meridional overturning circulation at 26.5°N. Science 317, 935–938. doi:10.1126/science.1141304.

Davis, R.E., Regier, L.A., Dufour, J., Webb, D.C., 1992. The Autonomous Lagrangian Circulation Explorer (ALACE). J. Atmosph. Oceanic Technol. 9, 264.

Dengg, J., Boening, C., Ernst, U., Redler, R., Beckmann, A., 1999. Effects of an improved model representation of overflow water on the subpolar North Atlantic. WOCE Newsl. 37, 10–15.

Dengler, M., Fischer, J., Schott, F.A., Zantopp, R., 2006. Deep Labrador Current and its variability in 1996–2005. Geophys. Res. Lett. 33. doi:10.1029/2006GL026702.

Doney, S.C., Jenkins, W.J., 1994. Ventilation of the Deep Western Boundary Current and Abyssal Western North Atlantic: estimates from tritium and ^{3}He distributions. J. Phys. Oceanogr. 24, 638.

Ducet, N., Traon, P.-Le, Reverdin, G., 1999. How accurately can we map the mesoscale ocean surface variability from the combination of T/P and ERS-1/2. Int. WOCE Newsl. 37, 40–43.

Eden, C., Boening, C., 2002. Sources of eddy kinetic energy in the Labrador Sea. J. Phys. Oceanogr. 32, 3346–3363. doi:10.1175/1520-0485(2002)032(3346:SOEKEI)2.0.CO;2.

Elliott, B., Sanford, T., 1986a. The subthermocline lens D1. Part I: description of water properties and velocity profiles. J. Phys. Oceanogr. 16, 532–548.

Elliott, B., Sanford, T., 1986b. The subthermocline lens D1. Part II: kinematics and dynamics. J. Phys. Oceanogr. 16, 549–561.

Fischer, J., Schott, F.A., 2002. Labrador Sea Water tracked by profiling floats—from the boundary current into the open North Atlantic. J. Phys. Oceanogr. 32, 573–584.

Fischer, J., Schott, F.A., Dengler, M., 2004. Boundary circulation at the exit of the Labrador Sea. J. Phys. Oceanogr. 34, 1548–1570 doi:10.1175/1520-0485(2004)034(1548:BCATEO)-2.0.CO;2.

Fratantoni, D.M., 2001. North Atlantic surface circulation during the 1990s observed with satellite-tracked drifters. J. Geophys. Res. 106, 22067–22093.

Furey, H., Bower, A., 2009. Export pathways from the subpolar North Atlantic: DLD2 RAFOS Float Data Report July 2003–November 2008. WHOI Tech. Report WHOI-2009-06, 166 pp.

Gary, S.F., Lozier, M.S., Boning, C.W., Biastoch, A., 2011. Deciphering the pathways for the deep limb of the Meridional Overturning Circulation. Deep-Sea Res. II 58 (17-18), 1781–1797.

Getzlaff, K., Boening, C.W., Dengg, J., 2006. Lagrangian perspectives of deep water export from the subpolar North Atlantic. Geophys. Res. Lett. 33. doi:10.1029/2006GL026470.

Hakkinen, S., Rhines, P.B., 2004. Decline of subpolar North Atlantic Circulation during the 1990s. Science 304, 555–559. doi:10.1126/science.1094917.

Heywood, K.J., McDonagh, E.L., White, M.A., 1994. Eddy kinetic energy of the North Atlantic subpolar gyre from satellite altimetry. J. Geophys. Res. 99, 22525–22539. doi:10.1029/94JC01740.

Hogg, N.G., 1992. On the transport of the Gulf Stream between Cape Hatteras and the Grand Banks. Deep-Sea Res. 39, 1231–1246.

Kalnay, E.M., Kanamitsu, M., Kistler, R., Collins, W., Deaven, D., Gandin, L., Iredell, M., Saha, S., White, G., Woollen, J., Zhu, Y., Chelliah, M., Ebisuzaki, W., Higgins, W., Janowiak, J., Mo, K.C., Ropelewski, C., Wang, J., Leetmaa, A., Reynolds, R., Jenne, R., Joseph, D., 1996. The NCEP/NCAR 40-year reanalysis project. Bull. Am. Meteorol. Soc. 77, 437–471.

Kearns, E.J., Rossby, H.T., 1998. Historical position of the North Atlantic Current. J. Geophys. Res. 103, 15509–15524.

Kieke, D., Rhein, M., Stramma, L., Smethie, W.M., LeBel, D.A., Zenk, W., 2006. Changes in the CFC inventories and formation rates of Upper Labrador Sea Water, 1997–2001. J. Phys. Oceanogr. 36, 64–86. doi:10.1175/JPO2814.1.

Kieke, D., Klein, B., Stramma, L., Rhein, M., Koltermann, K.P., 2009. Variability and propagation of Labrador Sea Water in the southern subpolar North Atlantic. Deep-Sea Res. I 56, 1656–1674. doi:10.1016/j.dsr.2009.05.010.

Kröger, J., 2001. Mechanismen meridionaler Transporte im tropischen Atlantik. Dissertation, Univ. Kiel, Kiel, Germany.

Lavender, K.L., Davis, R.E., Owens, W.B., 2000. Mid-depth recirculation observed in the interior Labrador and Irminger seas by direct velocity measurements. Nature 407, 66–69.

Lavender, K.L., Owens, W.B., Davis, R.E., 2005. The mid-depth circulation of the subpolar North Atlantic Ocean as measured by subsurface floats. Deep-Sea Res. I 52, 767–785. doi:10.1016/j.dsr.2004.12.007.

Lazier, J.R.N., Wright, D.G., 1993. Annual velocity variations in the Labrador Current. J. Phys. Oceanogr. 23, 659–678.

Lozier, M.S., 1997. Evidence for large-scale eddy-driven gyres in the North Atlantic. Science 277, 361–364.

Lozier, M.S., Owens, W.B., Curry, R.G., 1995. The climatology of the North Atlantic. Prog. Oceanogr. 36, 1–44.

McCartney, M.S., 1992. Recirculating components to the deep boundary current of the Northern North Atlantic. Prog. Oceanogr. 9, 283–383.

Petrie, B., Buckley, J., 1996. Volume and freshwater transport of the Labrador Current in Flemish Pass. J. Geophys. Res. 101, 28335–28342. doi:10.1029/96JC02779.

Pickart, R.S., Watts, D.R., 1990. Deep Western Boundary Current variability at Cape Hatteras. J. Mar. Res 48, 765–791.

Rhein, M., Weiss, R.F., Mertens, C., Min, D.H., Fleischmann, U., Putzka, A., Fischer, J., Smethie, W.M., Smythe-Wright, D., 2002. Labrador Sea Water: pathways, CFC inventory, and formation rates. J. Phys. Oceanogr. 32, 648–665.

Rio, M.-H., Hernandez, F., 2004. A mean dynamic topography computed over the world ocean from altimetry, in situ measurements, and a geoid model. J. Geophys. Res. 109, C12032.

Rossby, H.T., 1996. The North Atlantic Current and surrounding waters: at the crossroads. Rev. Geophys. 34, 463–481.

Rossby, H.T., Dorson, D., Fontaine, J., 1986. The RAFOS system. J. Atmos. Ocean. Technol. 3, 672–679.

Schott, F., Zantopp, R., Stramma, L., Dengler, M., Fischer, J., Wibaux, M., 2004. Circulation and deep water export at the western exit of the subpolar North Atlantic. J. Phys. Oceanogr. 34, 817–817-843.

Schott, F.A., Fischer, J., Dengler, M., Zantopp, R., 2006. Variability of the Deep Western Boundary Current east of the Grand Banks. Geophys. Res. Lett. 33. doi:10.1029/2006GL026563.

Shaw, P., Rossby, H.T., 1984. Towards a Lagrangian description of the Gulf Stream. J. Phys. Oceanogr. 14, 528–540.

Smethie Jr., W.M., Fine, R.A., Putzka, A., Jones, E.P., 2000. Tracing the flow of North Atlantic Deep Water using chlorofluorocarbons. J. Geophys. Res. 105, 14297–14324. doi:10.1029/1999JC900274.

Stommel, H., Arons, A.G., 1960a. On the abyssal circulation of the World Ocean—II. An idealized model of the circulation pattern and amplitude in oceanic basins. Deep-Sea Res. 6, 217–233.

Stommel, J., Arons, A.B., 1960b. On the abyssal circulation of the World Ocean—I. Stationary planetary flow patterns on a sphere. Deep-Sea Res. 6, 140–154.

Stramma, L., Kieke, D., Rhein, M., Schott, F., Yashayaev, I., Koltermann, K.P., 2004. Deep water changes at the western boundary of the subpolar North Atlantic during 1996 to 2001. Deep-Sea Res. I 51, 1033–1056.

Swift, D., Riser, S., 1994. RAFOS floats: defining and targeting surfaces of neutral buoyancy. J. Atmos. Ocean. Technol. 11, 1079–1092.

Talley, L.D., McCartney, M.S., 1982. Distribution and circulation of Labrador Sea Water. J. Phys. Oceanogr. 12, 1189–1205.
Treguier, A.M., Theetten, S., Chassignet, E.P., Penduff, T., Smith, R., Talley, L., Beismann, J.O., Boning, C., 2005. The North Atlantic subpolar gyre in four high-resolution models. J. Phys. Oceanogr. 35, 757–774.
Willebrand, J., Barnier, B., Boning, C., Dieterich, C., Killworth, P.D., Le Provost, C., Jia, Y., Molines, J., New, A.L., 2001. Circulation characteristics in three eddy-permitting models of the North Atlantic. Prog. Oceanogr. 48, 123–161.
Worthington, L.V., 1976. On the North Atlantic Circulation. Oceanographic Studies, 6. The Johns Hopkins University, Baltimore, MD, pp. 1–110.
Zenk, W., Pinck, A., Becker, S., Tillier, P., 2000. The Float Park: a new tool for a cost-effective collection of Lagrangian time series with dual release RAFOS floats. J. Atmos. Ocean. Technol. 17, 1439–1443.